

1 **Measurement Report: Effects of anthropogenic emissions and**
2 **environmental factors on biogenic secondary organic aerosol**
3 **(BSOA) formation in a coastal city of Southeastern China**

4
5 Youwei Hong^{a,b,c,d*}, Xinbei Xu^{a,b,c}, Dan Liao^e, Taotao Liu^{a,b,c}, Xiaoting Ji^{a,b,c}, Ke Xu^{a,b,d},
6 Chunyang Liao^f, Ting Wang^g, Chunshui Lin^g, Jinsheng Chen^{a,b,c*}

7

8 ^aCenter for Excellence in Regional Atmospheric Environment, Institute of Urban Environment,
9 Chinese Academy of Sciences, Xiamen, 361021, China

10 ^bKey Lab of Urban Environment and Health, Institute of Urban Environment, Chinese Academy
11 of Sciences, Xiamen, 361021, China

12 ^cUniversity of Chinese Academy of Sciences, Beijing, 100049, China

13 ^dSchool of Life Sciences, Hebei University, Baoding, 071000, China

14 ^eCollege of Environment and Public Health, Xiamen Huaxia University, Xiamen 361024, China

15 ^fState Key Laboratory of Environmental Chemistry and Ecotoxicology, Research Center for Eco-
16 Environmental Sciences, Chinese Academy of Sciences, Beijing 100085, China

17 ^g Institute of Earth Environment, Chinese Academy of Sciences, Xi'an, 710061, China

18

19 *Corresponding author E-mail: Jinsheng Chen (jschen@iue.ac.cn); Youwei Hong
20 (ywhong@iue.ac.cn)

21

22

23

24

25

26

27

28

29

30

31

32

33

34 **Abstract:**

35 To better understand the formation of biogenic secondary organic aerosol (BSOA),
36 aerosol samples with a 4 h time resolution were collected during summer and
37 wintertime in the southeast of China, along with on-line measurements of trace gases,
38 aerosol chemical compositions, and meteorological parameters. The samples were
39 analyzed by gas chromatography-mass spectrometry for PM_{2.5}-bound SOA tracers,
40 including isoprene (SOA_I), α/β -pinene (SOA_M), β -caryophyllene (SOA_C), and toluene
41 (ASOA). The average concentrations of total SOA tracers in winter and summer were
42 38.8 and 111.9 ng m⁻³, respectively, with the predominance of SOA_M (70.1% and
43 45.8%), followed by SOA_I (14.0% and 45.6%), ASOA (11.0% and 6.2%) and SOA_C
44 (4.9% and 2.3%). Compare to those in winter, the majority of BSOA tracers in summer
45 showed significant positive correlations with Ox (O₃+NO₂), HONO, ultraviolet (UV)
46 and temperature (T), indicating the influence of photochemical oxidation under
47 relatively clean conditions. However, in winter, BSOA tracers were significantly
48 correlated with PM_{2.5}, NO₃⁻, SO₄²⁻, and NH₃, attributed to the contributions of
49 anthropogenic emissions. Major BSOA tracers in both seasons was linearly correlated
50 with aerosol acidity (pH), liquid water content (LWC) and SO₄²⁻. The results indicated
51 that acid-catalyzed reactive uptake onto sulfate aerosol particles enhanced the
52 formation of BSOA. In summer, the clean air mass originated from the ocean, and
53 chlorine depletion was observed. We also found that concentrations of the total SOA
54 tracers was correlated with HCl and chlorine ions in PM_{2.5}, reflecting the contribution
55 of Cl-initiated VOC oxidations to the formation of SOA. In winter, the northeast
56 dominant wind direction brought continental polluted air mass to the monitoring site,
57 affecting the transformation of BSOA tracers. This implied that anthropogenic
58 emissions, atmospheric oxidation capacity and halogen chemistry have significant
59 effects on the formation of BSOA in the southeast coastal area.

60 **Keywords:** SOA tracers; biogenic volatile organic compounds; anthropogenic
61 pollutants; atmospheric oxidation capacity; coastal area

62

63 **1. Introduction**

64 Secondary organic aerosol (SOA) has attracted widespread scientific researchers
65 concerns, due to its potential impacts on climate change, human health and air quality
66 (Shrivastava et al., 2017; Reid et al., 2018; Zhu et al., 2019; Wang et al., 2021b).
67 Understanding the formation of SOA and assessing its relevance for environmental
68 effects become an integral part of aerosol chemistry (Charan et al., 2019; Xiao et al.,
69 2020; Palmer et al., 2022). However, due to its complex precursors and atmospheric
70 physical or chemical processes, SOA prediction by air quality models remains highly
71 uncertain (McFiggans et al., 2019). Therefore, it is necessary to better explore missed
72 SOA sources and unknown SOA formation mechanisms.

73 SOA was produced by the conversion of biogenic and anthropogenic volatile
74 organic compounds (BVOCs and AVOCs) through complex homogeneous and
75 heterogeneous reactions (Charan et al., 2019; Xiao et al., 2020; Mahilang et al., 2021).
76 BVOCs are the main precursors of SOA on a global scale, while AVOCs are the
77 predominant contributor to SOA in urban areas (Hallquist et al., 2009; Wang et al.,
78 2021a). Recently, laboratory, field observation and model studies have shown that
79 anthropogenic emissions greatly affect the formation of BSOA (Hoyle et al., 2011;
80 Shrivastava et al., 2019; Zhang et al., 2019b; Zhang et al., 2019c; Mahilang et al., 2021;
81 Xu et al., 2021). Anthropogenic air pollutants, such as NO_x, SO₂, NH₃ and aerosols,
82 could influence the conversion of BVOCs to the particulate phase and the production
83 of nitrogen and sulfur compounds (Wang et al., 2020). NO_x is one of the important
84 drivers of SOA formation and yields during both daytime and nighttime through
85 alternating the fate of peroxy radicals (RO₂·) (Sarrafzadeh et al., 2016; Newland et al.,
86 2021). While ·OH dominates the photochemical oxidation of BVOC during daylight
87 hours, and NO₃· becomes one of the main oxidants for biogenic SOA and organic
88 nitrates at night. SO₂ also plays an important role in changing SOA formation from
89 BVOC photooxidation and ozonolysis through sulfuric acid formation and acid-
90 catalyzed heterogeneous reactions (Zhao et al., 2018; Zhang et al., 2019b; Xu et al.,

91 2021). In addition, NH₃ and amines can affect the SOA yields and composition through
92 both gas-phase and heterogeneous reactions, by reacting with sulfuric or nitric acid to
93 generate secondary inorganic aerosols (SIA) (Ma et al., 2018; Liu et al., 2021; Lv et
94 al.,2022). However, due to complex precursors and atmospheric processes, the
95 combined effects of anthropogenic emissions and meteorological factors on the
96 formation of SOA are not fully understood.

97 The coastal area of southeastern China is under the East Asian monsoon control,
98 which cause an obvious alternation of polluted and clean air masses from continental
99 and ocean area, respectively (Wu et al., 2019; Hong et al., 2021). Also, the local
100 geographical environment, including relatively high humidity, dense vegetation and
101 strong atmospheric oxidation capacity, provides a good chance to study the sources and
102 formation mechanisms of SOA. In our previous studies, ground-based observations in
103 a mountainous forest area of this region showed that BSOA tracers were the largest
104 contributor to SOA, and the aerosols were highly oxidized (Hong et al., 2019). However,
105 with the development of rapid urbanization, anthropogenic emissions will be of great
106 significance on SOA formation (Liu et al., 2020). Halogen radicals (chlorine, bromine,
107 iodine) have an important role in tropospheric oxidants chemistry and OA formation
108 (Wang et al., 2021c). Therefore, it is necessary to investigate the sources and formation
109 mechanisms of SOA in coastal urban areas, and so as to provide a scientific basis for
110 the estimation of regional SOA budgets and PM_{2.5} pollution control.

111 In this study, a continuous PM_{2.5} sampling campaign with a 4 h time resolution
112 was conducted in a coastal city of southeastern China during the winter and
113 summertime period. Seasonal, diurnal variations and SOC contributions of SOA tracers
114 were analyzed. We also demonstrated the indications of SOA tracers for air pollution
115 process. Finally, the combined effects of anthropogenic emissions and major
116 environmental factors on promoting SOA formation was discussed.

117 **2. Materials and methods**

118 *2.1 Sample collection*

119 The sampling was performed at the Institute of Urban Environment, Chinese
120 Academy of Sciences (118.06° E, 24.61° N), which is located in a suburban area of
121 Xiamen, a coastal city of southeastern China. Detailed information of the air monitoring
122 supersite was described in our previous study (Hong et al., 2021). Briefly, time-resolved
123 (00:00–08:00, 08:00–12:00, 12:00–16:00, 16:00–20:00, 20:00–24:00 CST – China
124 Standard Time) PM_{2.5} samples were collected on the rooftop of the station (about 70m
125 above the ground). The sampling was carried out by using a high volume (1.05 m³ min⁻¹)
126 sampler (TH-1000C, Wuhan Tianhong, China) with a PM_{2.5} inlet from 10 to 18 January,
127 and from 5 to 14 July 2020. All samples were collected onto pre-baked (450 °C, 6 h)
128 quartz fiber filters. Field blank samples were also collected. The sample filters were
129 separately sealed in aluminum foil and stored in a freezer (–20 °C) prior to analysis.

130 2.2 SOA tracers analysis by GC/MS

131 The isoprene-derived SOA (SOA_I) tracers included 2 methyltetrols (MTLs: 2-
132 methylthreitol (MTL1) and 2-methylerythritol (MTL2)), C5-alkene triols (cis-2-
133 methyl-1,3,4-trihydroxy-1-butene, trans-2-methyl-1,3,4-trihydroxy-1-butene, and 3-
134 methyl-2,3,4-trihydroxy-1-butene) and 2-methylglyceric acid (MGA). The
135 monoterpene-derived SOA (SOA_M) tracers were composed of pinic acid (PA), pinonic
136 acid (PNA), 3-hydroxyglutaric acid (HGA), 3-methyl-1,2,3-butanetricarboxylic acid
137 (MBTCA), 3-hydro-4,4-dimethylglutaric acid (HDMGA), and 3-acetylglutaric acid
138 (AGA). The β-caryophyllene-derived SOA (SOA_C) tracer was β-caryophyllenic acid
139 (CA), the toluene-derived SOA (SOA_A) tracer was 2,3-Dihydroxy-4-oxopentanoic acid
140 (DHOPA) and levoglucosan (LEV) as a tracer of biomass burning. Due to the lack of
141 authentic standards, surrogate standards (including erythritol, malic acid, PA and
142 citramalic acid) were used to compensate for unavoidable assay variance of quantify
143 SOA_I, SOA_M, SOA_C and SOA_A tracer, in each sample during the pretreatment process,
144 respectively (Fu et al., 2009). ~~Details of SOA tracer's calculated concentrations based~~
145 ~~on relative response factors (RRFs) were presented in our previous studies (Hong et al.,~~
146 ~~2019; Liu et al., 2020).~~

147 The analytical procedure of fifteen SOA tracers was published in our previous

带格式的: 字体: (中文)+中文正文(宋体), 字体颜色: 自动设置

带格式的: 字体颜色: 自动设置

带格式的: 字体: 小四, 字体颜色: 自动设置

带格式的: 字体颜色: 自动设置

148 studies (Hong et al., 2019; Liu et al., 2020). Briefly, the filter samples were
149 ultrasonically extracted with a mixture of dichloromethane and methanol (2:1, v/v) for
150 10 min three times. The mixed extracts were filtered with a PTFE filter (0.22 μm), and
151 dried with high purity N_2 (99.99%), and then derivatized with 60 μL of
152 N,O-bis-(trimethylsilyl) trifluoroacetamide (BSTFA) with 1% trimethylsilyl chloride
153 and 10 μL of pyridine at 70 $^\circ\text{C}$ for 3 h. At last, 140 μL of internal standard solution (^{13}C
154 n-alkane solution, 1.507 $\text{ng } \mu\text{L}^{-1}$) was added into the samples. Then, relative response
155 factors (RRFs) of surrogate and internal standard were calculated to quantify the
156 targeted organic tracers in each sample. Details of SOA tracer's calculated
157 concentrations based on ~~relative response factors (RRFs)~~ were presented in our
158 previous studies (Hong et al., 2019; Liu et al., 2020).

带格式的: 字体: (中文) 宋体, 小四, 字体颜色: 自动设置

带格式的: 字体: (中文) 宋体

159

160 Fifteen SOA tracers were determined by GC-MSD (7890A/5975C, Agilent
161 Technologies, Inc., USA) with a DB-5 MS silica capillary column (i.d. 30 \times 0.25 mm,
162 0.25 μm film thickness). 1 μL sample was injected with splitless mode and high purity
163 helium (99.999%) was used as carrier gas at a stable flow of 1.0 mL/min. The GC
164 temperature was initiated at 100 $^\circ\text{C}$ (held for 1 min) and then to 300 $^\circ\text{C}$ at 5 $^\circ\text{C } \text{min}^{-1}$,
165 and kept at 300 $^\circ\text{C}$ for 10 min. The operation mode is electron ionization (EI) mode of
166 70 eV. The method detection limits (MDLs) for erythritol and PNA were 0.01 and 0.02
167 $\text{ng } \text{m}^{-3}$, respectively. The recoveries of erythritol, PNA, malic acid, PA and citramalic
168 acid were 67 \pm 2%, 73 \pm 1%, 75 \pm 1%, 88 \pm 7% and 82 \pm 8%, respectively. SOA tracers were
169 not detected in the field blank samples.

170 2.3 Observations in the air monitoring supersite

171 Water-soluble inorganic ions (WSII) in $\text{PM}_{2.5}$ (Cl^- , SO_4^{2-} , NO_3^- , Na^+ , K^+ , NH_4^+ ,
172 Mg^{2+} , and Ca^{2+}) and gas pollutants (HCl, HONO, HNO_3 , NH_3) were hourly measured
173 using a monitoring device for aerosols and gases in ambient Air (MARGA 2080;
174 Metrohm Applikon B.V.; Delft, Netherlands). Internal calibration was carried out using
175 LiBr standard solutions. The detection limit of Cl^- , SO_4^{2-} , NO_3^- , Na^+ , K^+ , NH_4^+ , Mg^{2+} ,
176 and Ca^{2+} were 0.01, 0.04, 0.05, 0.05, 0.09, 0.05, 0.06 and 0.09 $\mu\text{g } \text{m}^{-3}$, respectively.

177 Hourly mass concentrations of PM_{2.5} and PM₁₀ were measured by using a tapered
178 element oscillating microbalance (TEOM1405, Thermo Scientific Corp., MA, USA).
179 NO₂, SO₂, and O₃ were monitored using continuous gas analyzers (TEI 42i, 43i, and
180 49i, Thermo Scientific Corp., MA, USA). Ambient meteorological parameters
181 including relative humidity (RH), temperature (T), wind speed (WS), and wind
182 direction (WD) were obtained by an ultrasonic anemometer (150WX, Airmar, the
183 USA). Photolysis frequencies were determined using a photolysis spectrometer (PFS-
184 100, Focused Photonics Inc., Hangzhou, China), including the photolysis rate constants
185 $J(\text{O}^1\text{D})$, $J(\text{HCHO}_M)$, $J(\text{HCHO}_R)$, $J(\text{NO}_2)$, $J(\text{H}_2\text{O}_2)$, $J(\text{HONO})$, $J(\text{NO}_3_M)$ and
186 $J(\text{NO}_3_R)$, and the spectral band ranged from 270 to 790 nm. Boundary layer height
187 (BLH) based on ERA-5 reanalysis dataset was downloaded from the following link
188 <https://www.ecmwf.int/en/forecasts/datasets/reanalysis-datasets/era5>.

189 2.4 Estimation of SOC using a tracer-based method

190 The fraction of SOC formed by the oxidation of monoterpene, isoprene, β -
191 caryophyllene and toluene was estimated using a tracer-based method (Kleindienst et
192 al., 2007; Hong et al., 2019). It is defined as $[\text{SOC}] = \sum i[\text{tri}]/f_{\text{SOC}}$, where [SOC]
193 represents the mass concentration of SOC ($\mu\text{gC m}^{-3}$) and $\sum i[\text{tri}]$ means the sum of the
194 concentration of individual SOA tracer ($\mu\text{g m}^{-3}$). The carbon mass fractions (f_{SOC}) of
195 monoterpene, isoprene, β -caryophyllene and toluene were 0.231 ± 0.111 , $0.155 \pm$
196 0.114039 , 0.023 ± 0.005 and 0.008 ± 0.003 , respectively, based on smog-chamber
197 experimental data (Kleindienst et al., 2007).

198 2.5 Aerosol acidity and OH calculation

199 ~~The E-AIM-IV (Extended Aerosol Inorganic Model IV version) was used to~~
200 ~~simulate the aqueous and solid phases of ionic compositions in the mixing system (H^+ -~~
201 ~~NH_4^+ - SO_4^{2-} - NO_3^- - Cl^- - Na^+ - H_2O) at a given T and RH (Friese and Ebel, 2010).~~
202 ~~According to our previous study (Wu et al., 2020), the hourly averaged T, RH, SO_4^{2-} ,~~
203 ~~NO_3^- , Cl^- , NH_4^+ , Na^+ and molar concentrations of total aerosol acidity ($\text{H}^+_{\text{total}}$) were~~
204 ~~used as the input in the model E-AIMIV to obtain the concentrations of free ions~~

带格式的: 字体颜色: 浅蓝

205 (including free H^+ (H^+_{insitu}) in the aqueous phase, and liquid water content (LWC)).
 206 H^+_{insitu} defined as the moles of free hydrogen ions in the aqueous phase of aerosols per
 207 unit of air ($nmol \cdot m^{-3}$), is the actual acidity in the droplets of the aerosols. The H^+_{total}
 208 was estimated from the ionic balance of the relevant ionic species: $H^+_{total} =$
 209 $2SO_4^{2-} + NO_3^- + Cl^- - NH_4^+ - Na^+$.

210 The pH of aerosol was calculated as the follow:

$$211 \quad pH = -\lg\left(\frac{\gamma \times H^+_{insitu}}{V_{aq}/1000}\right)$$

212 where γ and V_{aq} denote the activity coefficient and the volume of particle aqueous
 213 phase in air ($cm^3 \cdot m$).

214 The forward mode of ISORROPIA II thermodynamic model was used to
 215 calculate the aerosol acidity (pH) (Fountoukis and Nenes, 2007) run by assuming that
 216 aerosol solutions were metastable (only a liquid phase). ISORROPIA II can calculate
 217 liquid water content (LWC), based on total SO_4^{2-} , NO_3^- , Cl^- , ammonia, non-volatile
 218 cations (Na^+ , K^+ , Ca^{2+} , Mg^{2+}), and meteorological factors (RH and T) (Rumsey et al.,
 219 2014; Guo et al., 2016). The pH value from ISORROPIA II was calculated using the
 220 following equation:

$$221 \quad pH = -\lg\left(\frac{1000 \times H^+}{LWC}\right)$$

222 where H^+ is the equilibrium particle hydronium ion concentration loading for an
 223 per volume air sample ($\mu g/m^3$).

224 The OH concentration ([OH]) was estimated using the NO_2 and HONO
 225 concentrations and the photolysis rate constants (J) of NO_2 , O_3 , and HONO, according
 226 to the following improved empirical formula (Wen et al., 2019).

$$227 \quad [OH] = 4.1 \times 10^9 \times \frac{J(O^1D)^{0.83} \times J(NO_2)^{0.19} \times (140 \times NO_2 + 1) + HONO \times J(HONO)}{0.41 \times NO_2^2 + 1.7 \times NO_2 + 1 + NO \times k_{NO+OH} + HONO \times k_{HONO+OH}}$$

228 2.6 Statistical analysis

229 Correlation analysis by SPSS 22.0 software (IBM, Armonk, NY, USA) was used
 230 to study the relationship among SOA tracers, meteorological parameters and criteria air

带格式的: 字体颜色: 浅蓝

带格式的: 字体颜色: 浅蓝

带格式的: 字体: (默认) Times New Roman, 小四, 字体颜色: 浅蓝

带格式的: 字体颜色: 浅蓝

带格式的: 字体: (默认) Times New Roman, 小四, 字体颜色: 浅蓝

带格式的: 字体颜色: 浅蓝

带格式的: 字体颜色: 浅蓝

带格式的: 字体颜色: 浅蓝

带格式的: 字体颜色: 浅蓝, 上标

带格式的: 字体颜色: 浅蓝

231 pollutants. One-way analysis of variance (ANOVA) was adopted to examine the
232 variations of different factors.

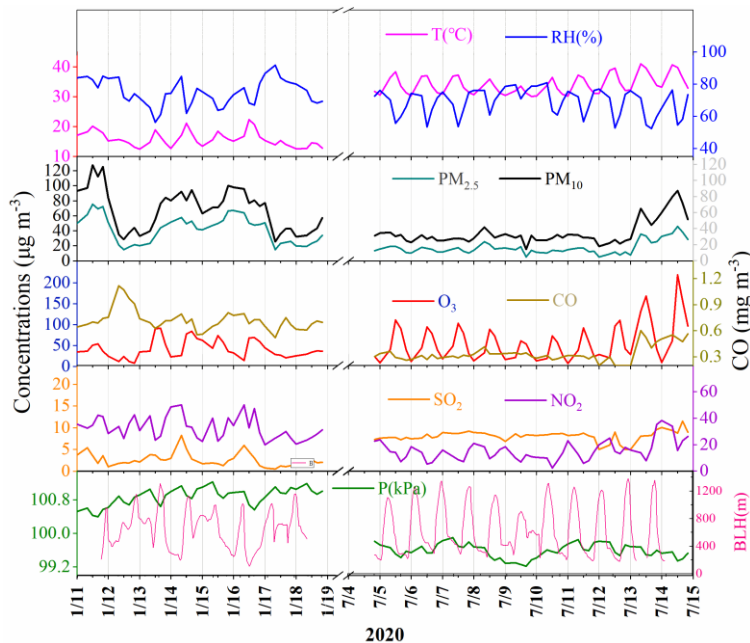
233 2.7. Backward trajectory analysis

234 Hybrid Single-Particle Lagrangian Integrated Trajectory (HYSPLIT) was used to
235 analyze the impacts of air masses on Xiamen during different seasons. 72 h backward
236 trajectories were calculated every hour at a height of 500 m. The meteorological data
237 with a resolution of 1° longitude \times 1° latitude was obtained from the NCEP/GDAS.
238 Cluster analysis was adopted using the total spatial variance (TSV).

239 3 Results and discussion

240 3.1. Overview of air pollutants

241 The concentrations of criteria air pollutants, including SO_2 , CO, NO_2 , O_3 , $\text{PM}_{2.5}$
242 and PM_{10} , and meteorological parameters during wintertime and summertime were
243 shown in Fig.1. The concentrations of $\text{PM}_{2.5}$ in winter ranged from 14.9 to $75.3 \mu\text{g m}^{-3}$
244 with an average of $42.1 \mu\text{g m}^{-3}$, which was much higher than that (the average of 18.4
245 $\mu\text{g m}^{-3}$) in summer, ranging from 12.8 to $46.4 \mu\text{g m}^{-3}$. The concentrations of CO, NO_2
246 and PM_{10} showed similar seasonal trends to the pattern of $\text{PM}_{2.5}$. In contrast, O_3 had the
247 highest concentration in summer, which was attributed to the formation of
248 photochemical reaction under strong UV radiation and the weak titration of nitrogen
249 oxides. Meanwhile, the concentrations of SO_2 ($8.37 \pm 0.79 \mu\text{g m}^{-3}$) in summer was also
250 higher than that ($2.63 \pm 1.95 \mu\text{g m}^{-3}$) in winter, mainly attributed to the influence of coal
251 combustion and ship emissions. The monitoring site was located approximately 15 km
252 away from Xiamen port area and a coal-fired power plant ($4 \times 300 \text{ kW}$) in the south.
253 Southerly winds were prevailed in summer, which might cause the relative high
254 concentration of SO_2 in the monitoring site.



255

256 **Figure 1. Time series of criteria air pollutants and meteorological parameters**
 257 **during the sampling period**

258 *3.2 Temporal variations of SOA tracers and estimated SOC*

259 Temporal variations of individual SOA tracer are shown in Fig.S1. The average
 260 concentrations of total SOA tracers in winter and summer were 3837.8 ± 3 and 111.9 ± 3
 261 ng m^{-3} , respectively, with t . The predominance of SOA_M (26.6 ng m^{-3}), followed by
 262 ASOA (4.60 ng m^{-3}), SOA_I (4.35 ng m^{-3}) and SOA_C (1.76 ng m^{-3}) was observed in winter
 263 while SOA_I (54.4 ng m^{-3}) and SOA_M (47.8 ng m^{-3}) in summer were the main contributors
 264 to total SOA tracers, followed by ASOA (6.64 ng m^{-3}) and SOA_C (2.45 ng m^{-3}). The
 265 predominance of SOA_M , followed by SOA_I and SOA_C . In summer, BSOA tracers
 266 showed much higher concentrations in the daytime (149.3 ng m^{-3}) than in the nighttime
 267 (60.1 ng m^{-3}), while inverse results were observed in winter (30.4 ng m^{-3} and 35.0 ng
 268 m^{-3} in the daytime and nighttime, respectively). For example As shown in Table S2, in
 269 summer, SOA_I in the daytime ranged from 21.3 to 293.2 ng m^{-3} (average of
 270 $82.60 \pm 65.66.3 \text{ ng m}^{-3}$) and the concentrations of SOA_I ranging from 6.81 to 110.1

带格式的: 字体颜色: 浅蓝

带格式的: 字体颜色: 浅蓝

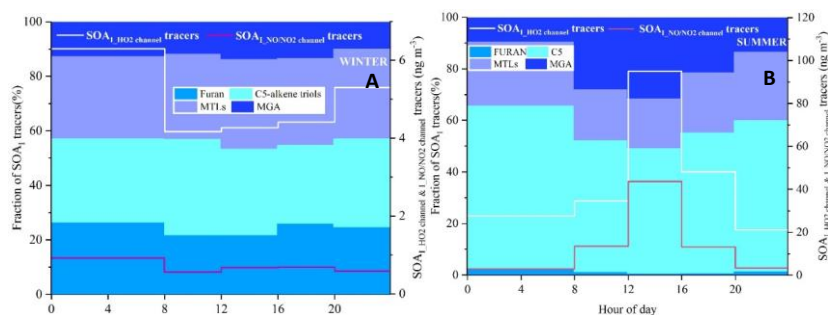
带格式的: 字体颜色: 浅蓝

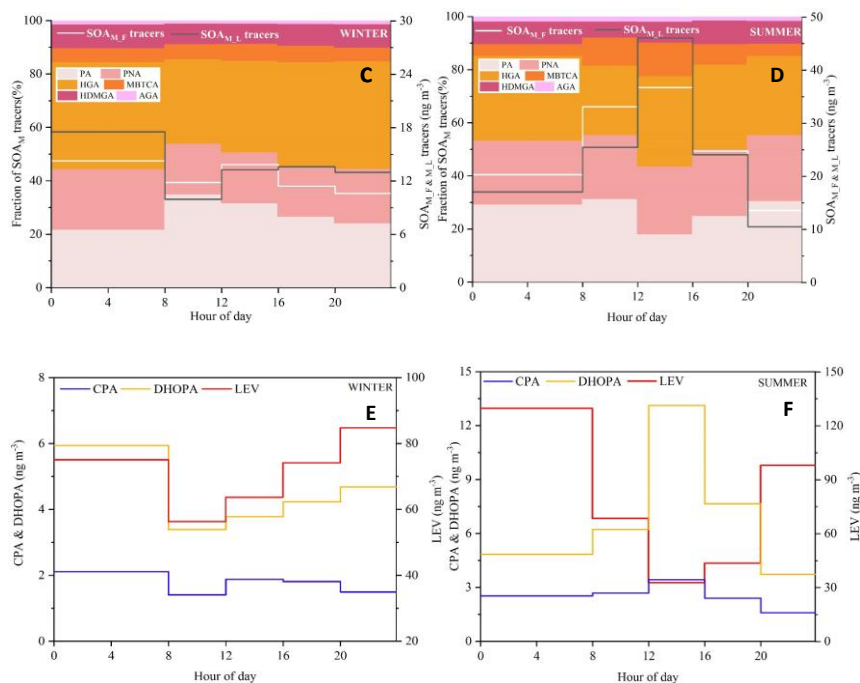
带格式的: 字体颜色: 浅蓝

带格式的: 字体颜色: 浅蓝

271 ng m^{-3} (average of $27.26.48 \pm 24.6 \text{ ng m}^{-3}$) were observed in the nighttime. However, in
 272 winter, the concentrations of isoprene SOA tracers in the daytime ranging from 1.36 to
 273 11.1 ng m^{-3} (average of $43.9379 \pm 2.62 \text{ ng m}^{-3}$) were lower than those (average of
 274 $15.34.91 \pm 83.32.75 \text{ ng m}^{-3}$) in the nighttime. As shown in Fig. 2, diurnal variations of
 275 SOA_M , SOA_I , CPA and DHOPA tracers in summer showed high levels in the afternoon
 276 (12:00–16:00 CST), due to the impacts of beneficial photochemical oxidation
 277 conditions caused by high temperature and strong UV radiation. The related SOA
 278 tracers were consisted with the emissions of their precursors including biogenic and
 279 anthropogenic VOCs, similar to our previous studies (Hong et al., 2019; Liu et al.,
 280 2020). However, the SOA tracers in winter showed the lowest concentrations in the
 281 morning (8:00–12:00 CST), related with the favorable dispersion conditions caused by
 282 the increasing planetary boundary layer height (BLH) (Fig.1). Levoglucosan (LEV), a
 283 typical tracer of biomass burning, similar seasonal and diurnal trend to other tracers was
 284 observed. However, LEV may not be as stable in the atmosphere, especially under high
 285 relative humidity conditions (Hoffmann et al., 2010). In this study, maybe, it's hard to
 286 reflect the real concentration of LEV. A correlation of CPA with LEV was carried out
 287 (Fig.S2), just to discuss the impacts of biomass burning on the distribution of CPA
 288 tracers through local or long-range transport. Totally, high concentrations of BSOA
 289 tracers was found in the daytime and in summer, indicating the effects of temperature
 290 on biogenic VOCs emissions and their photochemical oxidations. And the
 291 concentrations of BSOA tracers in winter increased in the nighttime, due to the
 292 changing of nocturnal boundary layer.

293





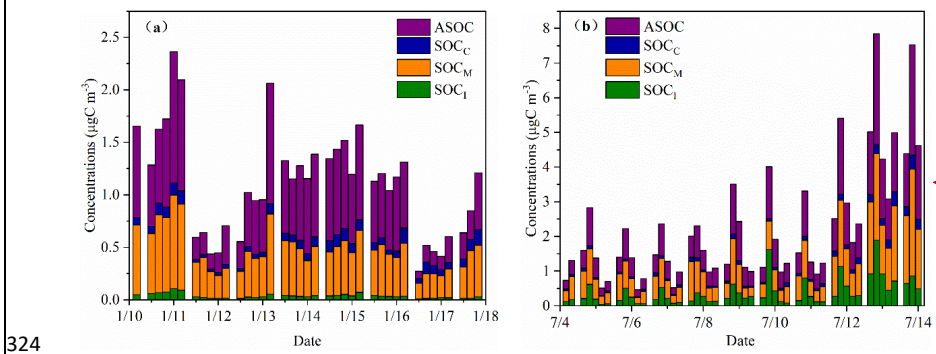
294

295

296 **Figure 2. Diurnal variation of individual SOA tracer during the wintertime and**
 297 **summertime**

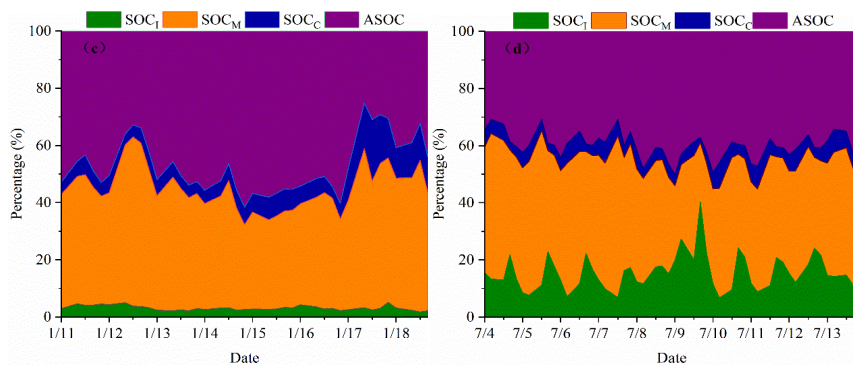
298 As shown in Fig.3a, b, SOA tracers-based SOC in winter and summer was
 299 estimated. The concentrations of SOC in winter ranged from 0.27 to 2.36 $\mu\text{g C m}^{-3}$, with
 300 an average of 1.11 $\mu\text{g C m}^{-3}$. Meanwhile, the concentrations of SOC in summer ranged
 301 from 0.46 to 7.85 $\mu\text{g C m}^{-3}$, with an average of 2.27 $\mu\text{g C m}^{-3}$. The concentrations of
 302 SOC in summer was higher than that in winter, attributed to the increase of flourishing
 303 vegetation emissions and photochemical reactions under high temperature and strong solar
 304 radiation conditions. ~~The results showed that the contributions of SOA tracers to SOC in~~
 305 ~~summer was higher than those in winter.~~ For individual SOA tracer, the concentrations
 306 of monoterpene-derived SOC ($0.87 \pm 0.64 \mu\text{g C m}^{-3}$) was comparable to the toluene-
 307 derived SOC ($0.90 \pm 0.69 \mu\text{g C m}^{-3}$), which were higher than isoprene-derived SOC
 308 ($0.39 \pm 0.38 \mu\text{g C m}^{-3}$) and β -caryophyllene-derived SOC ($0.10 \pm 0.08 \mu\text{g C m}^{-3}$). An
 309 obvious trend of diurnal variations of isoprene-derived SOC in summer was observed,

310 which was consistent with ~~a certain amount~~the diurnal pattern of isoprene
 311 concentration (Fig.S3) ~~emitted from various plants~~. However, no similar trend was
 312 found in winter~~—, attributed to the influence of low temperature on inhibiting the~~
 313 emissions of isoprene from various kinds of plants. In addition, the toluene,
 314 monoterpene, isoprene and β -caryophyllene-derived SOC in summer accounted for
 315 40.0%, 39.2%, 15.7% and 5.1% of the total SOC, respectively (Fig.3c, d). However, in
 316 winter, the percentages of toluene, monoterpene, isoprene and β -caryophyllene-derived
 317 SOC were 47.2%, 42.1%, 3.2% and 7.6%, respectively. The percentages of isoprene-
 318 derived SOC estimated from different precursors varied significantly among the
 319 seasons. High temperature enhanced the emissions of isoprene, and strong solar
 320 radiation favored the formation of isoprene SOA tracers, contributing to the highest
 321 isoprene-derived SOC percentage in summer (Ding et al., 2014). And the highest
 322 percentages of toluene-derived SOC (47.2%) in winter were related with anthropogenic
 323 emissions and adverse diffusion conditions.

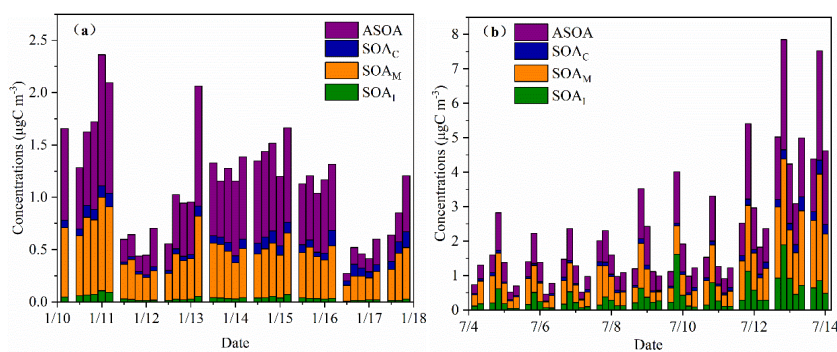


带格式的: 非突出显示
 带格式的: 非突出显示

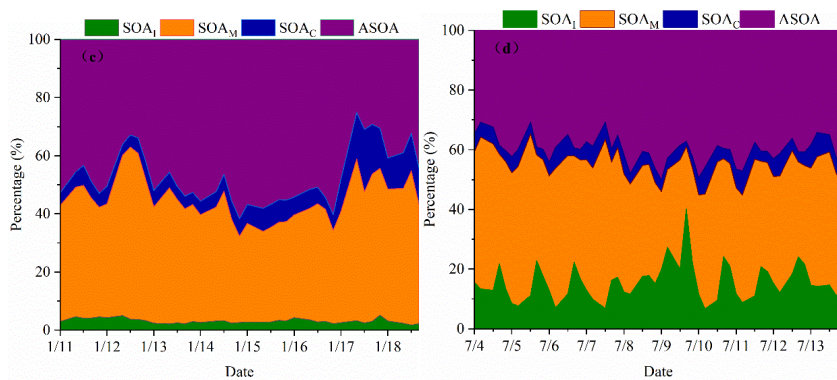
带格式的: 缩进: 首行缩进: 0 厘米



325



326



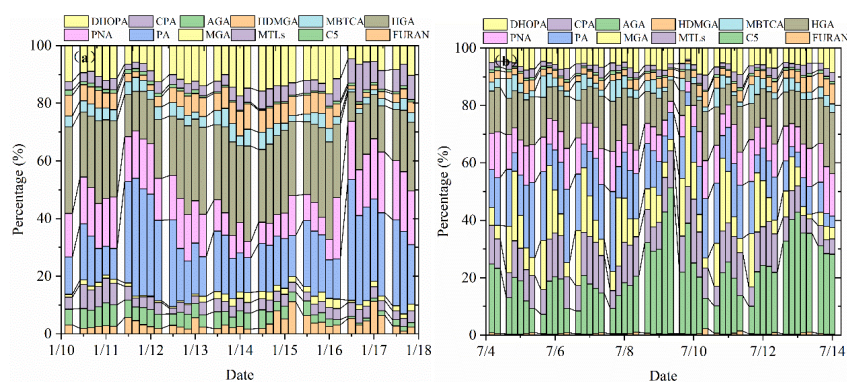
327

328 **Figure 3. Concentrations and percentages of SOA tracer-based estimated SOC**
 329 **during the sampling period**

330 *3.3 Atmospheric process indication of BSOA tracers*

331 As shown in Fig.4, percentages of different types of SOA tracers in winter and
 332 summer were calculated. In summer, the monoterpene, isoprene, toluene and β -

333 caryophyllene SOA tracers accounted for 45.8%, 45.6%, 6.2% and 2.3% of the total
 334 SOA tracers, respectively. However, in winter, the percentages of monoterpene,
 335 isoprene, toluene and β -caryophyllene SOA tracers were 70.1%, 14.0%, 11.0% and
 336 4.9%, respectively. The percentage of SOA_I tracers decreased sharply, due to the
 337 impacts of temperature on isoprene emissions, which was consisted with our previous
 338 findings (Hong et al., 2019). Meanwhile, the concentrations of SOA_M tracers were the
 339 largest in both seasons, due to a large amount of monoterpene emissions from the
 340 related plant species. Xiamen, an international garden city, located in coastal area of
 341 southeastern China. Monoterpene, such as α/β -pinene, is mostly emitted by coniferous
 342 plant and most flowers and fruits, while isoprene originates from broad-leaved trees
 343 and deciduous plants (Ding et al., 2014; Shrivastava et al., 2017; Yang et al., 2021).



344
 345 **Figure 4. Percentages of isoprene, monoterpene, β -caryophyllene and toluene**
 346 **SOA tracers in winter (a) and summer (b)**

347 ~~The α/β -pinene SOA tracers, including first (PA and PNA) and later generation~~
 348 ~~(HGA, AGA, HDMGA and MBTCA) products first-generation products (PA, PNA)~~
 349 ~~and later-generation products (HGA, AGA, HDMGA and MBTCA), could be were used~~
 350 to evaluate the aging degree of SOA_M BSOA (Ding et al., 2014; Hong et al., 2019). In
 351 this study, HGA (32.2%) was the major component of α/β -pinene tracers, followed by
 352 PA (30.5%), PNA (21.8%), HDMGA (7.3%), MBTCA (6.8%), and AGA (1.5%). The
 353 percentage of PA and PNA were much higher than those in mountainous background

带格式的: 字体: (默认) Times New Roman, 小四, 字体颜色: 自动设置

带格式的: 下标

354 areas (PA: 9% and PNA: 3%)(Hong et al., 2019), suggesting the contribution of
355 preliminary products to SOA in urban areas. As shown in Fig.4, the percentages of PA
356 and PNA in winter (21.8% and 14.2%) were higher than those in summer (14.2% and
357 10.7%). Reacted with atmospheric oxidants including O₃ and OH, PA and PNA were
358 transformed into MBTCA (Offenberg et al., 2007). This is the reason why the
359 proportions of PA and PNA had a significant decreasing trend from winter to summer.
360 The ratio of MBTCA/(PA+PNA) in summer and winter were 0.16±0.09 and 0.12±0.07,
361 respectively, which also proved the impacts of atmospheric oxidation capacity on the
362 aging degree of SOA_M. In addition, the ratio of HGA/MBTCA could be used to
363 distinguish the contribution of α-pinene or β-pinene to the SOA_M formation (Jaoui et
364 al., 2005; Ding et al., 2014). Low ratio of HGA/MBTCA (~1.0) showed that α-pinene
365 was the major precursor for SOA_M (Lewandowski et al., 2013). The ratio of
366 HGA/MBTCA with an average of 5.78 in Xiamen was high, suggesting the contribution
367 of β-pinene to SOA_M. ~~Low ratio of HGA/MBTCA (~1.0) showed that α-pinene was the~~
368 ~~major precursor for SOA_M (Lewandowski et al., 2013).~~

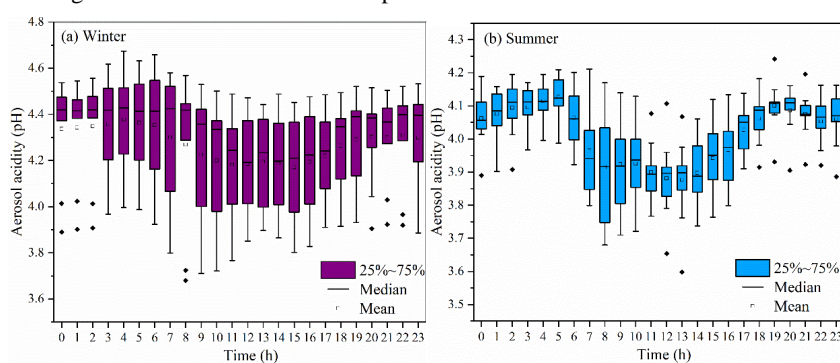
369 As shown in Fig.4, MTLs and C5 alkene triols were the main components of the
370 total SOA_I, with an average percentage of 68.0±14.9%, indicating a low-NO_x
371 environment (Ding et al., 2014; Liu et al., 2020). In summer, the percentages of MTLs
372 and C5 alkene triols to the total SOA tracers in summer (21.8% and 14.2%) were
373 obviously higher than those in winter (4.2% and 4.3%). This was consisted with the
374 fact that the concentrations of NO₂ (14.8±7.46 μg m⁻³) in summer was significantly
375 lower than that (32.7±32.6 μg m⁻³) in winter. Previous studies found that MTLs and C5
376 alkene triols were formed by the OH and HO₂ radicals via the HO₂ channel under low-
377 NO_x conditions (Surratt et al., 2010). C5 alkene triols are mainly produced by acid
378 catalyzed reaction of Isoprene Epoxydiols (IEPOX) in the gas phase, while MTLs are
379 formed by ring opening products of IEPOX (Surratt et al., 2007; Surratt et al., 2010).
380 And the ozonolysis of isoprene was also an important pathway for MTLs in the
381 presence of acid sulfate aerosols (Riva et al., 2016).

382 CPA, the typical tracer of sesquiterpenes, is formed by the photooxidation of β-

383 caryophyllene (Jaoui et al., 2007). As shown in Fig.4, CPA in winter and summer
 384 accounted for 5.0% and 2.3% of the total SOA tracers, respectively. This is because
 385 that the percentage of SOA_I has significant increase in summer. And the concentrations
 386 of CPA ($2.5 \pm 2.0 \text{ ng m}^{-3}$) in summer were higher than that ($1.7 \pm 0.8 \text{ ng m}^{-3}$) in winter,
 387 probably attributed to the emissions of β -caryophyllene driven by temperature and solar
 388 radiation. The CPA has a good correlation with DHOPA in summer (Fig.S2),
 389 suggesting the influence of photochemical oxidation (Liu et al., 2020). However, the
 390 CPA were not correlated with LEV in both seasons, reflecting the limited contribution
 391 of biomass burning (Zhang et al., 2019c).

392 3.4 Impacts of aerosol acidity on BSOA formation

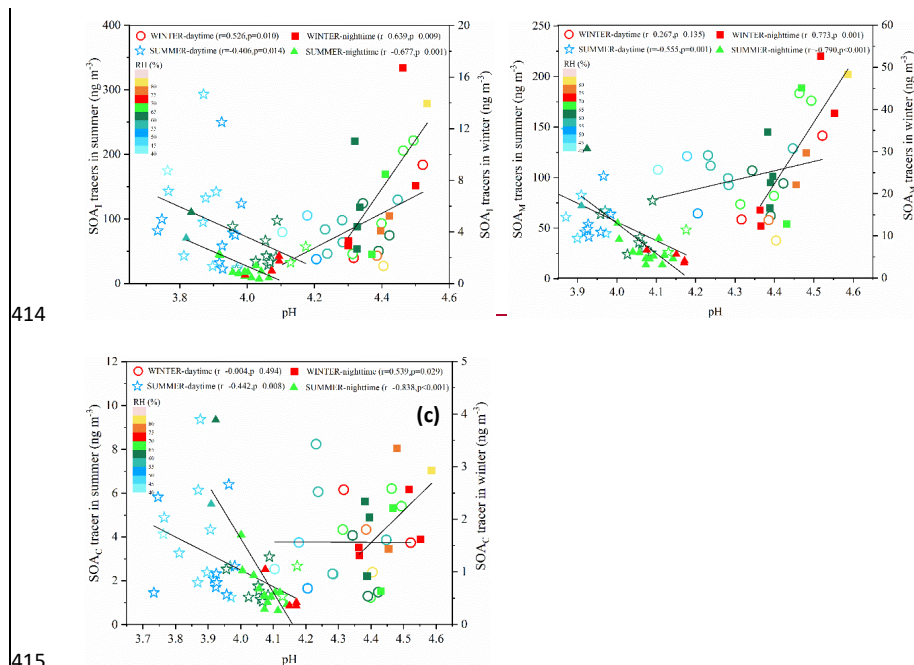
393 Aerosol acidity (pH) was an important factor on SOA formation (Surratt et al.,
 394 2007; Offenberg et al., 2009; Zhang et al., 2019b; Zhang et al., 2019d). Time series of
 395 aerosol pH calculated by ISORROPIA II is shown in Fig.5. The PM_{2.5} in Xiamen was
 396 moderately acidic with daily pH range from 3.68 to 4.67. The highest aerosol pH was
 397 observed in winter, and the lowest pH in summer. This is with similar seasonal trend,
 398 closing to the Yangtze River Delta (YRD) region, but obviously lower levels than those
 399 in NCP cities of China (Zhou et al., 2021). In general, the aerosol pH in Chinese cities
 400 were higher than those in US and European.



401

402 **Figure 5. Diurnal variations of aerosol acidity (pH) during the wintertime and**
 403 **summertime period (The boxes with error bars represent the 10th, 25th, 75th,**
 404 **and 90th percentiles)**

405 A declining trend pH during the daytime was observed (Fig. 5), which was related
 406 to the changes of chemical compositions and environmental conditions. The aerosol pH
 407 levels (~3 to 6) was related with a shift from sulfate- to nitrate-dominated aerosols (Guo
 408 et al., 2017). According to the multiphase buffer theory, the peak buffer pH (pKa*)
 409 regulated the aerosol pH, and temperature could obviously cause the variation of
 410 aerosol pH (Zheng et al., 2020). To further discuss the impacts of aerosol acidity on
 411 BSOA formation in coastal city, we analyzed the relationship between BSOA tracers
 412 and seed particles with different pH and liquid water content (LWC) (Fig. 6-S4 and
 413 Table 1).



416 **Figure 6. Correlations of SOA₁ tracers (a), SOA_M tracers (b), SOA_C tracer (c)**
 417 **with aerosol acidity (pH) during the daytime and night-time**

418 In Table 1, the BSOA tracers was linearly correlated with aerosol acidity (pH) and
 419 SO₄²⁻. In summer, BSOA tracers in the particle phase were found to increase with
 420 increasing acidity, which was attributed to the presence of acid catalyzed aerosols. For
 421 example, isoprene SOA tracers is mainly formed through acid-catalyzed reactive

422 uptake of isoprene-derived epoxydiols (IEPOX) onto sulfate aerosol particles.

Table 1. Correlations between individual BSOA tracer and environmental factors in winter and summer

Season	SOA tracer	pH	LWC	HONO	PM _{2.5}	Cl ⁻	NO ₂ ⁻	SO ₄ ²⁻	NH ₃	SO ₂	NO ₂	O ₃	T	RH	UV
WINTER (n=39)	C5	.584**	.701**	.534**	.690**	.569**	.710**	.663**	.705**	.308	.353*	.203	.361*	.0140	.200
	MTLs	.590**	.705**	.431*	.665**	.639**	.707**	.651**	.757**	.185	.229	.098	.353*	.0295	-.0068
	MGA	.390*	.707**	.0261	.668**	.081	.758**	.572**	.0284	.172	.123	.374*	.377*	-.0019	.238
	PA	.432**	.403**	.463**	.407**	.481*	.416*	.488*	.440*	.446*	.071	-.193	.319*	-.0205	.145
	PNA	.489**	.579**	.0311	.459**	.516**	.573**	.533**	.543**	.008	.071	-.101	.0121	.337*	-.122
	HGA	.443*	.829**	.352*	.834**	.600**	.847**	.754**	.641**	.275	.299	.451**	.451**	.0043	.210
	MBTCA	.433*	.678**	.447**	.670**	.435*	.733**	.589**	.710**	.327*	.253	.492**	.552**	-.0158	.0317
	HDMGA	.421*	.876**	.401*	.867**	.631**	.884**	.813**	.643**	.335*	.321*	.526**	.485**	-.0049	.0327
	AGA	.570**	.575**	.370*	.488**	.577**	.566**	.544**	.731**	.0126	.126	.019	.0279	.0298	-.0122
	CPA	.0212	.462**	-.0068	.452**	.483**	.437*	.419*	.255	-.015	-.170	.016	.0079	.0200	-.0144
SUMMER (n=50)	C5	-.495**	.425**	.0160	.622**	-.340*	.0268	.625**	.436**	.254	.025	.649**	.573**	-.529**	.0247
	MTLs	-.551**	.0131	.0055	.0272	-.439**	.0131	.428**	.304*	.089	-.0278	.550**	.610**	-.594**	.0263
	MGA	-.540**	.0029	.0116	.0132	-.403**	.0066	.472**	.0270	.096	-.410**	.443**	.633**	-.668**	.382*
	PA	-.633**	.483**	.601**	.461**	-.0135	.541**	.502**	.405*	.037	.038	.456**	.626**	-.558**	.400*
	PNA	-.664**	.616**	.387**	.812**	-.389**	.450**	.784**	.503**	.269	.294*	.769**	.718**	-.631**	.404*
	HGA	-.607**	.612**	.299*	.836**	-.384**	.447**	.770**	.539**	.316*	.272	.808**	.670**	-.599**	.0322
	MBTCA	-.752**	.415**	.0237	.577**	-.382**	.359*	.636**	.501**	.201	-.052	.712**	.852**	-.816**	.588**
	HDMGA	-.525**	.618**	.299*	.833**	-.342*	.408**	.768**	.488**	.358*	.365**	.746**	.574**	-.500**	.0240
	AGA	-.684**	.592**	.447**	.766**	-.334*	.479**	.735**	.435**	.244	.244	.694**	.720**	-.634**	.477**
	CPA	-.552**	.625**	.441**	.780**	-.280*	.453**	.763**	.307*	.299*	.299*	.611**	.529**	-.458**	.0305

*/ **Correlation coefficients with an asterisk indicate statistically significant relationships at $\alpha = 0.05$, and two asterisks mean significant at $\alpha = 0.01$.

427 In our previous studies, we have reported that high concentration of MTLs was related
428 with sulfate, which could significantly promote the formation of isoprene-SOA tracers
429 (Liu et al., 2020). Other studies also found that sulfate could increase the BSOA
430 production by promoting acid-catalyzed ring-opening reactions (Xu et al., 2015). In
431 contrast, positive correlations between BSOA tracers and aerosol pH in winter were
432 observed, indicating that the formation of BSOA was predominantly enhanced by other
433 factors, except for the aerosol acidity. The aerosol pH in winter was higher than those
434 in summer, probably due to the influence of nitrate-dominated aerosols. Also, the aged
435 aerosols through long-range transport might result in the increase of BSOA tracers and
436 aerosol pH.

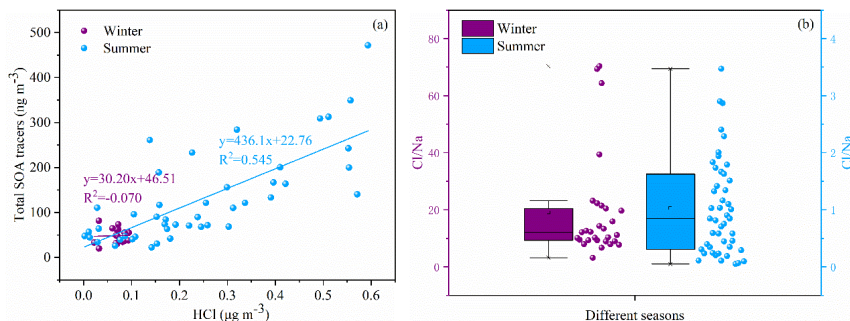
437 In addition, positive correlation between BSOA tracers and LWC was observed
438 (Table 1), probably attributed to the effects of the LWC on determining the peak buffer
439 pH (pKa*). Zheng et al. (2020) reported that the buffering effect of ammonia suppresses
440 the contribution of different chemical compositions in aerosol particles, making LWC
441 the primary determinant of aerosol pH. Other studies have demonstrated that the uptake
442 coefficient of first-generation oxidation products, especially for carbonyl compounds,
443 might depend on RH (Luo et al., 2019). Meanwhile, high LWC could reduce the aerosol
444 particle viscosity, which was benefit to the generation of the reactive intermediate such
445 as IEPOX, or other oxidation products of VOC into aqueous-phase of aerosol particles,
446 thereby promoting the formation of BSOA (Zhang et al., 2019b; Zhang et al., 2019d).

447 3.5 Impacts of chlorine on BSOA formation

448 Halogen radicals (Cl, Br and I) originated from sea salt aerosol (SSA) have an
449 important role in tropospheric oxidants chemistry (Wang et al., 2021c). In this study,
450 chlorine depletion was frequently observed in summer (Fig. 7a6b), indicating that HCl
451 can be formed through acid displacement of sea salt aerosol Cl^- by H_2SO_4 and HNO_3
452 produced from anthropogenic emissions of SO_2 and NO_x . Moreover, concentrations of
453 the total SOA tracers were positively correlated with HCl (Fig. 7a6a), suggesting the
454 enhancement of SOA precursors transformation. Previous studies have found that Cl-
455 initiated VOC oxidations could contribute to the formation of SOA (Wang and Ruiz,
456 2017; Dhulipala et al., 2019).

带格式的: 缩进: 首行缩进: 0 厘米

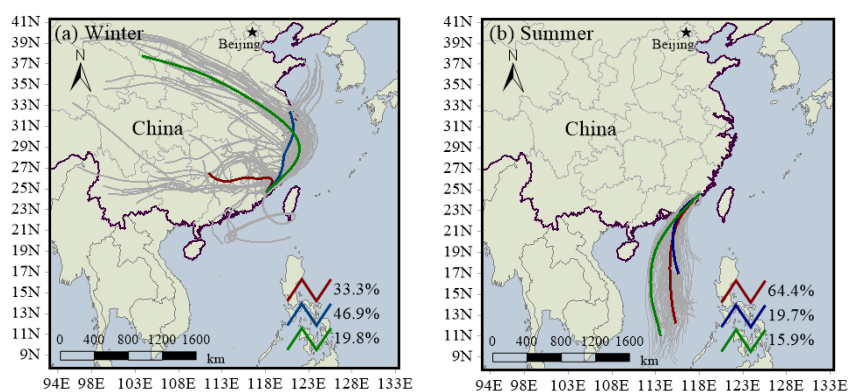
带格式的: 左侧: 3.17 厘米, 右侧: 3.17 厘米, 节的起始
位置: 连续, 无网格



457

458 **Figure 76. Correlations of total SOA tracers and HCl (a) and chlorine depletion**
 459 **(b) in different seasons**

460 Under ammonia-rich conditions, HCl partitioned into the aqueous particulate
 461 phase mostly took place, and chlorine ions could affect aqueous oxidation of secondary
 462 organic compounds (Xu et al., 2021). As shown in Table 1, ~~the correlations of most of~~
 463 ~~SOA tracers in winter were correlated with found to increase with the increasing~~
 464 ~~concentrations of NH₃ and~~ chlorine ions in PM_{2.5}, while inverse results were observed
 465 in summer. In winter, the dominant wind direction is northeast (Fig. 87), and chlorine
 466 mainly come from continental polluted air mass, such as industrial and combustion
 467 emissions. So, anthropogenic pollutants through long-range transport might cause the
 468 enhancement of SOA tracer concentrations at the monitoring site. However, in summer,
 469 negative correlations of BSOA tracers and chlorine ions in PM_{2.5} was found, probably
 470 due to the influence of chlorine depletion. As shown in Fig. 87, the dominant wind
 471 direction is southerly, and chlorine mainly originated from the spray of sea salt.



472

473 **Figure 87. Backward trajectories analyses during the winter (a) and summertime**
 474 **(b)**

475 *3.6. Enhanced formation of BSOA by anthropogenic emissions*

476 Recent studies had indicated that anthropogenic emissions might affect SOA
 477 formation through multiple chemical processes, based on laboratory studies and field
 478 observations (Kari et al., 2019; Shrivastava et al., 2019; Zhang et al., 2019c; Cheng et
 479 al., 2021; Xu et al., 2021). In this study, we conducted the correlation analysis of
 480 individual SOA tracers and O_3+NO_2 , HONO, OH, SO₂, NH₃, PM_{2.5}, sulfate,
 481 nitrate, as well as meteorological parameters (including T, RH and UV) (Table 1).

482 Most of SOA tracers have a significant positive correlation with NH₃, suggesting
 483 an enhancement effect on the formation of SOA (Table 1). NH₃ could affect the SOA
 484 yields through both gas-phase and heterogeneous reactions (Na et al., 2007; Ma et al.,
 485 2018; Hao et al., 2020). Gas-phase reaction between NH₃ and organic acids (such as
 486 PA and PNA) produced ammonium salts in the particle phase, which contributed to the
 487 increased SOA formation. However, not all gas-phase organic acids (e.g., MGA and
 488 pyruvic acid) could demonstrate gas-to-particle conversion (Na et al., 2007). When
 489 SOA formation had ceased, the addition of excessive NH₃ would result in the rapid
 490 decomposition of the main SOA species, due to the nucleophilic attack of NH₃ (Ma et
 491 al., 2018).

492

带格式的: 缩进: 首行缩进: 0.85 厘米

带格式的: 左侧: 3.17 厘米, 右侧: 3.17 厘米, 顶端: 2.54 厘米, 底端: 2.54 厘米, 节的起始位置: 连续, 宽度: 21 厘米, 高度: 29.7 厘米, 无网格

Table 1 Correlations between individual BSOA tracer and environmental factors in winter and summer

Season	SOA tracer	pH	$\frac{[O_3]}{[O_2]}$	HONO	PM _{2.5}	Cl ⁻	NO ₃ ⁻	SO ₄ ²⁻	NH ₃	S	NO ₂	O ₃	T	RH	UV
	CS	.58 4**	.70 1**	.53 4**	.69 0**	.56 0**	.71 0**	.66 2**	.70 5**	.03 08	.35 2*	.02 03	.36 1*	.01 40	.02 00
	MTH	.59 0**	.70 5**	.43 1*	.66 5**	.63 0**	.70 7**	.65 1**	.75 7**	.01 85	.02 29	.00 98	.35 3*	.02 95	.00 68
WIN FER (n=20)	MGA	.39 0*	.70 7**	.02 61	.66 8**	.00 81	.75 8**	.57 2**	.02 84	.01 72	.01 23	.37 4*	.37 7*	= 4*	.02 38
	PA	.43 2*	.40 3**	.46 3**	.40 7**	.48 1*	.41 6*	.48 8*	.44 0*	.44 6*	.02 41	= 93	.31 9*	= 05	.01 45
	PNA	.48 0**	.57 0**	.02 11	.45 0**	.51 6**	.57 2**	.53 2**	.54 2**	.00 8	.00 71	= 04	.01 21	.01 7*	= 01
	HGA	.44 2*	.82 9**	.25 2*	.82 4**	.60 0**	.84 7**	.75 4**	.64 1**	.02 75	.02 99	.45 1**	.45 1**	.00 43	.02 40

	MBT	.43	.67	.44	.67	.43	.73	.58	.71	.32	0.2	.49	.55	-	0.3
	CA	3*	8**	7**	0**	5*	3**	9**	0**	7*	53	2**	2**	0+ 58	17
	HDM	.43	.87	.40	.86	.62	.88	.81	.64	.22	.22	.52	.48	-	0.3
	GA	1*	6**	1*	7**	1**	4**	3**	3**	5*	1*	6**	5**	0+ 40	27
	AGA	.57	.57	.37	.48	.57	.56	.54	.73	0.1	0.1	0.0	0.2	0.2	0.1
	CPA	0.2	.46	-	.45	.48	.43	.41	0.2	0.1	0.1	0.0	0.0	0.2	0.1
		12	2**	0.0 68	2**	3**	7*	9*	55	5	70	16	79	00	44
	CS	.49	.42	0.1	.62	.24	0.2	.62	.43	0.2	0.0	.64	.57	-.52	0.2
		5**	5**	60	2**	0*	68	5**	6**	54	25	0**	2**	0**	47
	MTL	-.55	0.1	0.0	0.2	-.43	0.1	-.42	.30	0.0	-	.55	.61	-.59	0.2
		1**	31	55	72	9**	31	8**	4*	89	0.2 78	0**	0**	4**	63
	MGA	-.54	0.0	0.1	0.1	-.40	0.0	-.47	0.2	0.0	-.41	.44	.63	-.66	.38
		0**	29	16	22	2**	66	2**	70	96	0**	2**	2**	8**	2*
	PA	-.62	.48	.60	.46	-	.54	.50	.40	0.0	0.2	.45	.62	-.55	.40
		3**	3**	1**	1**	0.1 35	1**	2**	5*	37	38	6**	6**	8**	0*
	PNA	-.66	.61	.38	.81	-.38	.45	.78	.50	0.2	.29	.76	.71	-.63	.40
		4**	6**	7**	2**	0**	0**	4**	2**	69	4*	9**	8**	1**	4*
	MGA	-.60	.61	.29	.82	-.28	.44	.77	.52	.21	0.2	.80	.67	-.50	0.2
		7**	2**	9*	6**	4**	7**	0**	0**	6*	72	8**	0**	0**	22
	MBT	-.75	.41	0.2	.57	-.38	.35	.63	.50	0.2	-	.71	.85	-.81	.58
	CA	2**	5**	37	7**	2**	9*	6**	1**	01	0.0 52	2**	2**	6**	8**
	HDM	-.52	.61	.29	.82	-.34	.40	.76	.48	.35	.36	.74	.57	-.50	0.2
	GA	5**	8**	0*	2**	2*	8**	8**	8**	8*	5**	6**	4**	0**	40
	AGA	-.68	.59	.44	.76	-.22	.47	.72	.42	0.2	0.2	.69	.72	-.62	.47
		4**	2**	7**	6**	4*	9**	5**	5**	44	71	4**	0**	4**	7**
	CPA	-.55	.62	.44	.78	-.28	.45	.76	.30	.29	.50	.61	.52	-.45	0.2
		2**	5**	1**	0**	0*	3**	3**	7*	9*	3**	1**	9**	8**	05

***Correlation coefficients with an asterisk indicate statistically significant relationships at a = 0.05, and two asterisks mean significant at a = 0.01.

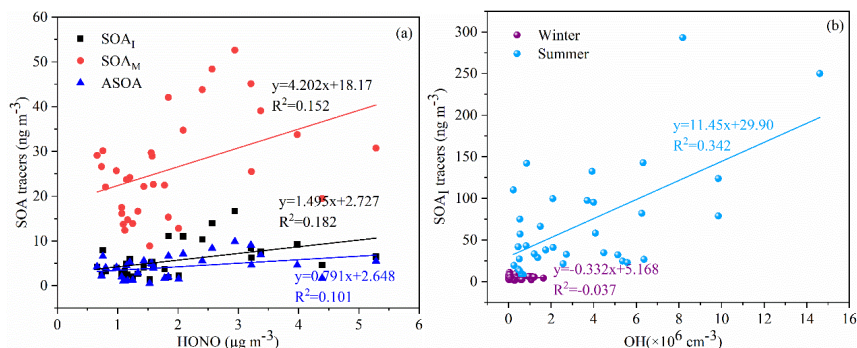


Figure 98. Relationships of SOA tracers and HONO and its estimated OH

带格式的: 居中

As an indicator of atmospheric oxidation capacity, the tropospheric odd oxygen Ox (O_3+NO_2) was calculated. As shown in Table 1, the majority of SOA tracers in summer showed significant positive correlations with Ox ($R>0.5$, $P<0.001$). However, in winter, a part of SOA_M tracers (e.g. HGA, MBTCA and HDMGA) were found to be significantly correlated with Ox. In addition, HONO and OH radicals, another critical indicator of atmospheric oxidation capacity, was also discussed. In this study, the concentration of OH radicals calculated from HONO in summer was higher than those in winter. In summer, the SOA_I tracers was correlated with OH radicals (Fig.9a8b); ~~consisted, consisted~~ with previous findings that OH radicals could promote the formation of SOA (Sarrafzadeh et al., 2016; Liu et al., 2019; Song et al., 2019; Zhang et al., 2019a). Due to its photolysis to produce OH radicals during the daytime, HONO could facilitate SOA formation. In winter, the concentrations of SOA_I, SOA_M and ASOA tracers were correlated with HONO (Fig.9a8a). These results indicated high concentrations of HONO and sufficient ultraviolet radiation could enhance the photochemical reactions of VOCs. Which was consisted with our previous results on the formation of peroxyacetyl nitrate (PAN) (Hu et al., 2020). As for T and UV, it exhibited significantly positive correlations with the related SOA tracers, especially in summer. These results suggested that SOA tracers were produced from the photo-oxidation of VOC precursors (Cheng et al., 2021).

In addition, the SOA tracers were significantly positive correlated with PM_{2.5} and its components including NO₃⁻ and SO₄²⁻. In coastal cities of southeastern China, with the development of rapid urbanization, air pollution caused by motor vehicles and industrial emissions is becoming more ~~and more obvious~~ frequent in winter (Wu et al.,

26 2020). The Xiamen port is one of the top 10 ports in China, resulting the impacts of
27 ship emissions and port activities on ambient air quality (Xu et al., 2018), and the
28 numbers of motor vehicles increased sharply in recent years. We also found that the
29 90th percentile of maximum daily average 8h (MDA8) O₃ concentrations in Xiamen
30 was significantly increased from 2015 to 2020 (Fig. S5). During the past several years,
31 the elevated sSecondary inorganic formation of components, including NO₃⁻, SO₄²⁻ and
32 NH₄⁺, PM_{2.5}-accounted for 60-70% of the total PM_{2.5} fine particle, and OM ranged
33 from 30% to 40%. NO₃⁻, SO₄²⁻ and NH₄⁺ are significant components of secondary
34 inorganic aerosols (Wu et al., 2019; Hong et al., 2021). These results also proved
35 implied the obvious effects of anthropogenic emissions and enhanced atmospheric
36 oxidation capacity on secondary formation of aerosol particles under atmospheric
37 stagnant conditions atmospheric relatively stability conditions during the winter.

38 Conclusions

39 Pollution characteristics and source identification of BSOA tracers during the
40 summer and winter in coastal areas of southeastern China were investigated. The
41 average concentration of total BSOA tracers in summer was higher than that in winter,
42 with the predominance of SOA_M, followed by SOA_I and SOA_C. The BSOA tracers in
43 summer were predominantly produced by the influence of photochemical oxidation
44 under relatively clean conditions. However, in winter, the formation of BSOA tracers
45 were attributed to the impacts of anthropogenic emissions and atmospheric stagnant
46 conditions, reflecting the anthropogenic biogenic interactions. In addition, the results
47 also indicated that acid-catalyzed reactive uptake onto sulfate aerosol particles
48 enhanced the formation of BSOA in both seasons. We further found that Cl-initiated
49 VOC oxidations has potentially accelerated the transformation of BSOA precursors
50 through sea salt aerosol originated from the ocean in summer and anthropogenic
51 emissions in winter. This study demonstrated that the combined effects of
52 anthropogenic pollutants and atmospheric oxidation capacity on the formation of
53 BSOA in coastal area.

54
55 **Data Availability.** The data set related to this work can be accessed via
56 <https://doi.org/10.5281/zenodo.6376025> (Hong, 2022). The details are also available
57 upon request from the corresponding author (ywhong@iue.ac.cn).

58
59
60
61
62
63
64
65
66
67
68
69
70
71
72
73
74
75
76
77
78
79
80
81
82
83
84
85
86
87
88
89
90
91
92
93

Authorship Contribution Statement. Youwei Hong and Xinbei Xu contributed equally to this work. Youwei Hong designed and wrote the manuscript. Xinbei Xu collected the data, contributed to the data analysis. Dan Liao, Taotao Liu, Xiaoting Ji and Ke Xu performed modeling analyses and data analysis. Jinsheng Chen supported funding of observation and research. Chunyang Liao, Ting Wang and Chunshui Lin contributed to revise the manuscript.

Competing interests. The authors declare that they have no conflict of interest.

Acknowledgement. The authors gratefully acknowledge Yanting Chen, Han Zhang and Xu Liao (Institute of Urban Environment, Chinese Academy of Sciences) for the guidance and assistance during sample pretreatment, and Lingling Xu and Mengren Li (Institute of Urban Environment, Chinese Academy of Sciences) for the discussion of this paper. This study was supported by Fujian Key Laboratory of Atmospheric Ozone Pollution Prevention and Xiamen Atmospheric Environment Observation and Research Station of Fujian Province (Institute of Urban Environment, Chinese Academy of Sciences).

Financial support. This research was financially supported by the Xiamen Youth Innovation Fund Project (3502ZZ20206094), the foreign cooperation project of Fujian Province (2020I0038), the Cultivating Project of Strategic Priority Research Program of Chinese Academy of Sciences (XDPB1903), the National Key Research and Development Program (2016YFC0112200), State Key Laboratory of Environmental Chemistry and Ecotoxicology, Research Center for Eco-Environmental Sciences, CAS (KF2020-06), the FJIRSM&IUE Joint Research Fund (RHZX-2019-006) and center for Excellence in Regional Atmospheric Environment project (EOL1B20201).

Reference

- 94
95 [Charan, S. M., Huang, Y., and Seinfeld, J. H.: Computational Simulation of Secondary](#)
96 [Organic Aerosol Formation in Laboratory Chambers, Chem. Rev., 119, 11912-11944,](#)
97 [10.1021/acs.chemrev.9b00358, 2019.](#)
- 98 [Cheng, Y., Ma, Y., and Hu, D.: Tracer-based source apportioning of atmospheric organic](#)
99 [carbon and the influence of anthropogenic emissions on secondary organic aerosol](#)
100 [formation in Hong Kong, Atmos. Chem. Phys., 21, 10589-10608, 10.5194/acp-21-](#)
101 [10589-2021, 2021.](#)
- 102 [Dhulipala, S. V., Bhandari, S., and Hildebrandt Ruiz, L.: Formation of oxidized organic](#)
103 [compounds from Cl-initiated oxidation of toluene, Atmospheric Environment, 199, 265-](#)
104 [273, 10.1016/j.atmosenv.2018.11.002, 2019.](#)
- 105 [Ding, X., He, Q.-F., Shen, R.-Q., Yu, Q.-Q., and Wang, X.-M.: Spatial distributions of](#)
106 [secondary organic aerosols from isoprene, monoterpenes, beta-caryophyllene, and](#)
107 [aromatics over China during summer, Journal of Geophysical Research-Atmospheres,](#)
108 [119, 11877-11891, 10.1002/2014jd021748, 2014.](#)
- 109 [Fountoukis, C., and Nenes, A.: ISORROPIA II: a computationally efficient](#)
110 [thermodynamic equilibrium model for \$K^+\$ - \$Ca^{2+}\$ - \$Mg^{2+}\$ - \$NH_4^+\$ - \$Na^+\$ - \$SO_4^{2-}\$ -](#)
111 [\$NO_3^-\$ - \$Cl^-\$ - \$H_2O\$ aerosols, Atmos. Chem. Phys., 7, 4639-4659, 10.5194/acp-7-](#)
112 [4639-2007, 2007.](#)
- 113 [Fu, P., Kawamura, K., Chen, J., and Barrie, L. A.: Isoprene, Monoterpene, and Sesquiterpene](#)
114 [Oxidation Products in the High Arctic Aerosols during Late Winter to Early Summer,](#)
115 [Environmental Science & Technology, 43, 4022-4028, 10.1021/es803669a, 2009.](#)
- 116 [Guo, H., Sullivan, A. P., Campuzano-Jost, P., Schroder, J. C., Lopez-Hilfiker, F. D.,](#)
117 [Dibb, J. E., Jimenez, J. L., Thornton, J. A., Brown, S. S., Nenes, A., and Weber,](#)
118 [R. J.: Fine particle pH and the partitioning of nitric acid during winter in the](#)
119 [northeastern United States, Journal of Geophysical Research: Atmospheres, 121,](#)
120 [10.355-310.376, <https://doi.org/10.1002/2016JD025311>, 2016.](#)
- 121 [Guo, H., Weber, R. J., and Nenes, A.: High levels of ammonia do not raise fine particle pH](#)
122 [sufficiently to yield nitrogen oxide-dominated sulfate production, Scientific Reports, 7,](#)
123 [12109, 10.1038/s41598-017-11704-0, 2017.](#)
- 124 [Hallquist, M., Wenger, J. C., Baltensperger, U., Rudich, Y., Simpson, D., Claeys, M.,](#)
125 [Dommen, J., Donahue, N. M., George, C., Goldstein, A. H., Hamilton, J. F., Herrmann,](#)
126 [H., Hoffmann, T., Iinuma, Y., Jang, M., Jenkin, M. E., Jimenez, J. L., Kiendler-Scharr,](#)
127 [A., Maenhaut, W., McFiggans, G., Mentel, T. F., Monod, A., Prevot, A. S. H., Seinfeld,](#)
128 [J. H., Surratt, J. D., Szmigielski, R., and Wildt, J.: The formation, properties and impact](#)
129 [of secondary organic aerosol: current and emerging issues, Atmospheric Chemistry and](#)
130 [Physics, 9, 5155-5236, 10.5194/acp-9-5155-2009, 2009.](#)
- 131 [Hao, L., Kari, E., Leskinen, A., Worsnop, D. R., and Virtanen, A.: Direct contribution of](#)
132 [ammonia to \$\alpha\$ -pinene secondary organic aerosol formation, Atmos. Chem. Phys., 20,](#)
133 [14393-14405, 10.5194/acp-20-14393-2020, 2020.](#)
- 134 [Hoffmann, D., Tilgner, A., Iinuma, Y., and Herrmann, H.: Atmospheric Stability of](#)
135 [Levogluconan: A Detailed Laboratory and Modeling Study, Environmental Science &](#)
136 [Technology, 44, 694-699, 10.1021/es902476f, 2010.](#)
- 137 [Hong, Y., Xu, X., Liao, D., Zheng, R., Ji, X., Chen, Y., Xu, L., Li, M., Wang, H., Xiao, H.,](#)
138 [Choi, S.-D., and Chen, J.: Source apportionment of PM2.5 and sulfate formation during](#)
139 [the COVID-19 lockdown in a coastal city of southeast China, Environmental Pollution,](#)
140 [286, 117577, <https://doi.org/10.1016/j.envpol.2021.117577>, 2021.](#)
- 141 [Hong, youwei. \(2022\). Dataset for ACP by Hong et al., 2022 \[Data set\]. Zenodo.](#)
142 [<https://doi.org/10.5281/zenodo.6376025>](#)
- 143 [Hong, Z., Zhang, H., Zhang, Y., Xu, L., Liu, T., Xiao, H., Hong, Y., Chen, J., Li, M., Deng,](#)
144 [J., Wu, X., Hu, B., and Chen, X.: Secondary organic aerosol of PM2.5 in a mountainous](#)

145 [forest area in southeastern China: Molecular compositions and tracers implication,](#)
146 [Science of the Total Environment, 653, 496-503, 10.1016/j.scitotenv.2018.10.370, 2019.](#)
147 [Hoyle, C. R., Boy, M., Donahue, N. M., Fry, J. L., Glasius, M., Guenther, A., Hallar, A. G.,](#)
148 [Hartz, K. H., Petters, M. D., Petaja, T., Rosenoern, T., and Sullivan, A. P.: A review of](#)
149 [the anthropogenic influence on biogenic secondary organic aerosol, Atmospheric](#)
150 [Chemistry and Physics, 11, 321-343, 10.5194/acp-11-321-2011, 2011.](#)
151 [Hu, B., Liu, T., Hong, Y., Xu, L., Li, M., Wu, X., Wang, H., Chen, J., and Chen, J.:](#)
152 [Characteristics of peroxyacetyl nitrate \(PAN\) in a coastal city of southeastern China:](#)
153 [Photochemical mechanism and pollution process, Science of the Total Environment,](#)
154 [719, 10.1016/j.scitotenv.2020.137493, 2020.](#)
155 [Jaoui, M., Kleindienst, T. E., Lewandowski, M., Offenberg, J. H., and Edney, E. O.:](#)
156 [Identification and quantification of aerosol polar oxygenated compounds bearing](#)
157 [carboxylic or hydroxyl groups. 2. Organic tracer compounds from monoterpenes,](#)
158 [Environmental Science & Technology, 39, 5661-5673, 10.1021/es048111b, 2005.](#)
159 [Jaoui, M., Lewandowski, M., Kleindienst, T. E., Offenberg, J. H., and Edney, E. O.: \$\beta\$ -](#)
160 [caryophyllinic acid: An atmospheric tracer for \$\beta\$ -caryophyllene secondary organic](#)
161 [aerosol, Geophysical Research Letters, 34, 10.1029/2006gl028827, 2007.](#)
162 [Kari, E., Hao, L. Q., Ylisirmio, A., Buchholz, A., Leskinen, A., Yli-Pirila, P., Nuutinen, I.,](#)
163 [Kuuspalo, K., Jokiniemi, J., Faiola, C. L., Schobesberger, S., and Virtanen, A.: Potential](#)
164 [dual effect of anthropogenic emissions on the formation of biogenic secondary organic](#)
165 [aerosol \(BSOA\), Atmospheric Chemistry and Physics, 19, 15651-15671, 10.5194/acp-](#)
166 [19-15651-2019, 2019.](#)
167 [Kleindienst, T. E., Jaoui, M., Lewandowski, M., Offenberg, J. H., Lewis, C. W., Bhave, P. V.,](#)
168 [and Edney, E. O.: Estimates of the contributions of biogenic and anthropogenic](#)
169 [hydrocarbons to secondary organic aerosol at a southeastern US location, Atmospheric](#)
170 [Environment, 41, 8288-8300, 10.1016/j.atmosenv.2007.06.045, 2007.](#)
171 [Lewandowski, M., Piletic, I. R., Kleindienst, T. E., Offenberg, J. H., Beaver, M. R., Jaoui, M.,](#)
172 [Docherty, K. S., and Edney, E. O.: Secondary organic aerosol characterisation at field](#)
173 [sites across the United States during the spring-summer period, International Journal of](#)
174 [Environmental Analytical Chemistry, 93, 1084-1103, 10.1080/03067319.2013.803545,](#)
175 [2013.](#)
176 [Liu, S., Tsona, N. T., Zhang, Q., Jia, L., Xu, Y., and Du, L.: Influence of relative humidity on](#)
177 [cyclohexene SOA formation from OH photooxidation, Chemosphere, 231, 478-486,](#)
178 [10.1016/j.chemosphere.2019.05.131, 2019.](#)
179 [Liu, S., Huang, D., Wang, Y., Zhang, S., Wu, C., Du, W., and Wang, G.: Synergetic effect of](#)
180 [NH₃ and NO_x on the production and optical absorption of secondary organic aerosol](#)
181 [formation from toluene photooxidation, Atmos. Chem. Phys. Discuss., 2021, 1-38,](#)
182 [10.5194/acp-2021-560, 2021.](#)
183 [Liu, T., Hu, B., Xu, X., Hong, Y., Zhang, Y., Wu, X., Xu, L., Li, M., Chen, Y., Chen, X., and](#)
184 [Chen, J.: Characteristics of PM_{2.5}-bound secondary organic aerosol tracers in a coastal](#)
185 [city in Southeastern China: Seasonal patterns and pollution identification, Atmospheric](#)
186 [Environment, 237, 10.1016/j.atmosenv.2020.117710, 2020.](#)
187 [Lowe, S., Jersey, J., Shoup, R., Garofolo, F., Savoie, N., Mortz, E., Needham, S., Caturla, M.](#)
188 [C., Steffen, R., Sheldon, C., Hayes, R., Samuels, T., Di Donato, L., Kamerud, J.,](#)
189 [Michael, S., Lin, Z. P., Hillier, J., Moussallie, M., Teixeira, L. D., Rocci, M., Buonarati,](#)
190 [M., Truog, J., Hussain, S., Lundberg, R., Breau, A., Zhang, T. Y., Jonker, J., Berger, N.,](#)
191 [Gagnon-Carignan, S., Nehls, C., Nicholson, R., Hilhorst, M., Karnik, S., de Boer, T.,](#)
192 [Houghton, R., Smith, K., Cojocar, L., Allen, M., Harter, T., Fatmi, S., Sayyarpour, F.,](#)
193 [Vija, J., Malone, M., and Heller, D.: Recommendations on: internal standard criteria,](#)
194 [stability, incurred sample reanalysis and recent 483s by the Global CRO Council for](#)
195 [Bioanalysis, Bioanalysis, 3, 1323-1332, 10.4155/Bio.11.135, 2011.](#)

196 [Luo, H., Jia, L., Wan, Q., An, T., and Wang, Y.: Role of liquid water in the formation of O-3](#)
197 [and SOA particles from 1,2,3-trimethylbenzene, Atmospheric Environment, 217,](#)
198 [10.1016/j.atmosenv.2019.116955, 2019.](#)

199 [Lv, S., Wang, F., Wu, C., Chen, Y., Liu, S., Zhang, S., Li, D., Du, W., Zhang, F., Wang, H.,](#)
200 [Huang, C., Fu, Q., Duan, Y., and Wang, G.: Gas-to-Aerosol Phase Partitioning of](#)
201 [Atmospheric Water-Soluble Organic Compounds at a Rural Site in China: An Enhancing](#)
202 [Effect of NH₃ on SOA Formation, Environmental Science & Technology,](#)
203 [10.1021/acs.est.1c06855, 2022.](#)

204 [Ma, Q., Lin, X. X., Yang, C. G., Long, B., Gai, Y. B., and Zhang, W. J.: The influences of](#)
205 [ammonia on aerosol formation in the ozonolysis of styrene: roles of Criegee intermediate](#)
206 [reactions, Roy Soc Open Sci, 5, ARTN 17217110.1098/rsos.172171, 2018.](#)

207 [Mahilang, M., Deb, M. K., and Pervez, S.: Biogenic secondary organic aerosols: A review on](#)
208 [formation mechanism, analytical challenges and environmental impacts, Chemosphere,](#)
209 [262, 10.1016/j.chemosphere.2020.127771, 2021.](#)

210 [McFiggans, G., Mentel, T. F., Wildt, J., Pullinen, I., Kang, S., Kleist, E., Schmitt, S.,](#)
211 [Springer, M., Tillmann, R., Wu, C., Zhao, D. F., Hallquist, M., Faxon, C., Le Breton, M.,](#)
212 [Hallquist, A. M., Simpson, D., Bergstrom, R., Jenkin, M. E., Ehn, M., Thornton, J. A.,](#)
213 [Alfarra, M. R., Bannan, T. J., Percival, C. J., Priestley, M., Topping, D., and Kiendler-](#)
214 [Scharr, A.: Secondary organic aerosol reduced by mixture of atmospheric vapours,](#)
215 [Nature, 565, 587-593, 10.1038/s41586-018-0871-y, 2019.](#)

216 [Na, K., Song, C., Switzer, C., and Cocker, D. R.: Effect of Ammonia on Secondary Organic](#)
217 [Aerosol Formation from \$\alpha\$ -Pinene Ozonolysis in Dry and Humid Conditions,](#)
218 [Environmental Science & Technology, 41, 6096-6102, 10.1021/es061956y, 2007.](#)

219 [Newland, M. J., Bryant, D. J., Dunmore, R. E., Bannan, T. J., Acton, W. J. F., Langford, B.,](#)
220 [Hopkins, J. R., Squires, F. A., Dixon, W., Drysdale, W. S., Ivatt, P. D., Evans, M. J.,](#)
221 [Edwards, P. M., Whalley, L. K., Heard, D. E., Slater, E. J., Woodward-Massey, R., Ye,](#)
222 [C., Mehra, A., Worrall, S. D., Bacak, A., Coe, H., Percival, C. J., Hewitt, C. N., Lee, J.](#)
223 [D., Cui, T., Surratt, J. D., Wang, X., Lewis, A. C., Rickard, A. R., and Hamilton, J. F.:](#)
224 [Low-NO atmospheric oxidation pathways in a polluted megacity, Atmos. Chem. Phys.,](#)
225 [21, 1613-1625, 10.5194/acp-21-1613-2021, 2021.](#)

226 [Offenberg, J. H., Lewis, C. W., Lewandowski, M., Jaoui, M., Kleindienst, T. E., and Edney,](#)
227 [E. O.: Contributions of toluene and alpha-pinene to SOA formed in an irradiated](#)
228 [toluene/alpha-pinene/NO_x/air mixture: Comparison of results using C-14 content and](#)
229 [SOA organic tracer methods, Environmental Science & Technology, 41, 3972-3976,](#)
230 [10.1021/es070089+, 2007.](#)

231 [Offenberg, J. H., Lewandowski, M., Edney, E. O., Kleindienst, T. E., and Jaoui, M.: Influence](#)
232 [of Aerosol Acidity on the Formation of Secondary Organic Aerosol from Biogenic](#)
233 [Precursor Hydrocarbons, Environmental Science & Technology, 43, 7742-7747,](#)
234 [10.1021/es901538e, 2009.](#)

235 [Palmer, P. I., Marvin, M. R., Siddans, R., Kerridge, B. J., and Moore, D. P.: Nocturnal](#)
236 [survival of isoprene linked to formation of upper tropospheric organic aerosol, Science,](#)
237 [375, 562-566, doi:10.1126/science.abg4506, 2022.](#)

238 [Reid, J. P., Bertram, A. K., Topping, D. O., Laskin, A., Martin, S. T., Petters, M. D., Pope, F.](#)
239 [D., and Rovelli, G.: The viscosity of atmospherically relevant organic particles, Nature](#)
240 [Communications, 9, 10.1038/s41467-018-03027-z, 2018.](#)

241 [Riva, M., Budisulistiorini, S. H., Zhang, Z., Gold, A., and Surratt, J. D.: Chemical](#)
242 [characterization of secondary organic aerosol constituents from isoprene ozonolysis in](#)
243 [the presence of acidic aerosol, Atmospheric Environment, 130, 5-13,](#)
244 [10.1016/j.atmosenv.2015.06.027, 2016.](#)

245 [Rumsey, I. C., Cowen, K. A., Walker, J. T., Kelly, T. J., Hanft, E. A., Mishoe, K.,](#)
246 [Rogers, C., Proost, R., Beachley, G. M., Lear, G., Frelink, T., and Otjes, R. P.:](#)
247 [An assessment of the performance of the Monitor for AeRosols and GAses in](#)

248 [ambient air \(MARGA\): a semi-continuous method for soluble compounds,](#)
249 [Atmos. Chem. Phys., 14, 5639-5658, 10.5194/acp-14-5639-2014, 2014.](#)
250 [Sarrafzadeh, M., Wildt, J., Pullinen, I., Springer, M., Kleist, E., Tillmann, R., Schmitt, S. H.,](#)
251 [Wu, C., Mentel, T. F., Zhao, D., Hastie, D. R., and Kiendler-Scharr, A.: Impact of NO_x](#)
252 [and OH on secondary organic aerosol formation from beta-pinene photooxidation,](#)
253 [Atmospheric Chemistry and Physics, 16, 11237-11248, 10.5194/acp-16-11237-2016,](#)
254 [2016.](#)
255 [Shrivastava, M., Cappa, C. D., Fan, J., Goldstein, A. H., Guenther, A. B., Jimenez, J. L.,](#)
256 [Kuang, C., Laskin, A., Martin, S. T., Ng, N. L., Petaja, T., Pierce, J. R., Rasch, P. J.,](#)
257 [Roldin, P., Seinfeld, J. H., Shilling, J., Smith, J. N., Thornton, J. A., Volkamer, R.,](#)
258 [Wang, J., Worsnop, D. R., Zaveri, R. A., Zelenyuk, A., and Zhang, Q.: Recent advances](#)
259 [in understanding secondary organic aerosol: Implications for global climate forcing,](#)
260 [Reviews of Geophysics, 55, 509-559, 10.1002/2016rg000540, 2017.](#)
261 [Shrivastava, M., Andreae, M. O., Artaxo, P., Barbosa, H. M. J., Berg, L. K., Brito, J., Ching,](#)
262 [J., Easter, R. C., Fan, J., Fast, J. D., Feng, Z., Fuentes, J. D., Glasius, M., Goldstein, A.](#)
263 [H., Alves, E. G., Gomes, H., Gu, D., Guenther, A., Jathar, S. H., Kim, S., Liu, Y., Lou,](#)
264 [S., Martin, S. T., McNeill, V. F., Medeiros, A., de Sa, S. S., Shilling, J. E., Springston, S.](#)
265 [R., Souza, R. A. F., Thornton, J. A., Isaacman-VanWertz, G., Yee, L. D., Ynoue, R.,](#)
266 [Zaveri, R. A., Zelenyuk, A., and Zhao, C.: Urban pollution greatly enhances formation of](#)
267 [natural aerosols over the Amazon rainforest, Nature Communications, 10,](#)
268 [10.1038/s41467-019-08909-4, 2019.](#)
269 [Song, M., Zhang, C., Wu, H., Mu, Y., Ma, Z., Zhang, Y., Liu, J., and Li, X.: The influence of](#)
270 [OH concentration on SOA formation from isoprene photooxidation, Science of the Total](#)
271 [Environment, 650, 951-957, 10.1016/j.scitotenv.2018.09.084, 2019.](#)
272 [Surratt, J. D., Lewandowski, M., Offenberg, J. H., Jaoui, M., Kleindienst, T. E., Edney, E. O.,](#)
273 [and Seinfeld, J. H.: Effect of acidity on secondary organic aerosol formation from](#)
274 [isoprene, Environmental Science & Technology, 41, 5363-5369, 10.1021/es0704176,](#)
275 [2007.](#)
276 [Surratt, J. D., Chan, A. W. H., Eddingsaas, N. C., Chan, M., Loza, C. L., Kwan, A. J., Hersey,](#)
277 [S. P., Flagan, R. C., Wennberg, P. O., and Seinfeld, J. H.: Reactive intermediates](#)
278 [revealed in secondary organic aerosol formation from isoprene, Proceedings of the](#)
279 [National Academy of Sciences of the United States of America, 107, 6640-6645,](#)
280 [10.1073/pnas.0911114107, 2010.](#)
281 [Wang, D. S., and Ruiz, L. H.: Secondary organic aerosol from chlorine-initiated oxidation of](#)
282 [isoprene, Atmos. Chem. Phys., 17, 13491-13508, 10.5194/acp-17-13491-2017, 2017.](#)
283 [Wang, J., Ye, J., Zhang, Q., Zhao, J., Wu, Y., Li, J., Liu, D., Li, W., Zhang, Y., Wu, C., Xie,](#)
284 [C., Qin, Y., Lei, Y., Huang, X., Guo, J., Liu, P., Fu, P., Li, Y., Lee, H. C., Choi, H.,](#)
285 [Zhang, J., Liao, H., Chen, M., Sun, Y., Ge, X., Martin, S. T., and Jacob, D. J.: Aqueous](#)
286 [production of secondary organic aerosol from fossil-fuel emissions in winter Beijing](#)
287 [haze, Proc Natl Acad Sci U S A, 118, 10.1073/pnas.2022179118, 2021a.](#)
288 [Wang, J., Ye, J., Zhang, Q., Zhao, J., Wu, Y., Li, J., Liu, D., Li, W., Zhang, Y., Wu, C., Xie,](#)
289 [C., Qin, Y., Lei, Y., Huang, X., Guo, J., Liu, P., Fu, P., Li, Y., Lee, H. C., Choi, H.,](#)
290 [Zhang, J., Liao, H., Chen, M., Sun, Y., Ge, X., Martin, S. T., and Jacob, D. J.: Aqueous](#)
291 [production of secondary organic aerosol from fossil-fuel emissions in winter Beijing](#)
292 [haze, Proceedings of the National Academy of Sciences of the United States of America,](#)
293 [118, 10.1073/pnas.2022179118, 2021b.](#)
294 [Wang, S., Du, L., Tsona, N. T., Jiang, X., You, B., Xu, L., Yang, Z., and Wang, W.: Effect of](#)
295 [NO_x and SO₂ on the photooxidation of methylglyoxal: Implications in secondary](#)
296 [aerosol formation, J Environ Sci \(China\), 92, 151-162, 10.1016/j.jes.2020.02.011, 2020.](#)
297 [Wang, X., Jacob, D. J., Downs, W., Zhai, S., Zhu, L., Shah, V., Holmes, C. D., Sherwen, T.,](#)
298 [Alexander, B., Evans, M. J., Eastham, S. D., Neuman, J. A., Veres, P. R., Koenig, T. K.,](#)
299 [Volkamer, R., Huey, L. G., Bannan, T. J., Percival, C. J., Lee, B. H., and Thornton, J. A.:](#)

300 [Global tropospheric halogen \(Cl, Br, I\) chemistry and its impact on oxidants, Atmos.](#)
301 [Chem. Phys., 21, 13973-13996, 10.5194/acp-21-13973-2021, 2021c.](#)
302 [Wen, L., Chen, T., Zheng, P., Wu, L., Wang, X., Mellouki, A., Xue, L., and Wang, W.:](#)
303 [Nitrous acid in marine boundary layer over eastern Bohai Sea, China: Characteristics,](#)
304 [sources, and implications, Sci. Total Environ., 10.1016/j.scitotenv.2019.03.225, 2019.](#)
305 [Wu, X., Xu, L. L., Hong, Y. W., Chen, J. F., Qiu, Y. Q., Hu, B. Y., Hong, Z. Y., Zhang, Y.](#)
306 [R., Liu, T. T., Chen, Y. T., Bian, Y. H., Zhao, G. Q., Chen, J. S., and Li, M. R.: The air](#)
307 [pollution governed by subtropical high in a coastal city in Southeast China: Formation](#)
308 [processes and influencing mechanisms, Science of the Total Environment, 692, 1135-](#)
309 [1145, 10.1016/j.scitotenv.2019.07.341, 2019.](#)
310 [Wu, X., Li, M., Chen, J., Wang, H., Xu, L., Hong, Y., Zhao, G., Hu, B., Zhang, Y., Dan, Y.,](#)
311 [and Yu, S.: The characteristics of air pollution induced by the quasi-stationary front:](#)
312 [Formation processes and influencing factors, Science of the Total Environment, 707,](#)
313 [10.1016/j.scitotenv.2019.136194, 2020.](#)
314 [Xiao, Y., Wu, Z., Guo, S., He, L., Huang, X., and Hu, M.: Formation mechanism of](#)
315 [secondary organic aerosol in aerosol liquid water: A review, Chinese Science Bulletin,](#)
316 [65, 3118-3133, 2020.](#)
317 [Xu, L., Du, L., Tsona, N. T., and Ge, M. F.: Anthropogenic Effects on Biogenic Secondary](#)
318 [Organic Aerosol Formation, Advances in Atmospheric Sciences, 38, 1053-1084,](#)
319 [10.1007/s00376-020-0284-3, 2021.](#)
320 [Xu, L., Guo, H. Y., Boyd, C. M., Klein, M., Bougiatioti, A., Cerully, K. M., Hite, J. R.,](#)
321 [Isaacman-VanWertz, G., Kreisberg, N. M., Knote, C., Olson, K., Koss, A., Goldstein, A.](#)
322 [H., Hering, S. V., de Gouw, J., Baumann, K., Lee, S. H., Nenes, A., Weber, R. J., and](#)
323 [Ng, N. L.: Effects of anthropogenic emissions on aerosol formation from isoprene and](#)
324 [monoterpenes in the southeastern United States, Proceedings of the National Academy of](#)
325 [Sciences of the United States of America, 112, 37-42, 10.1073/pnas.1417609112, 2015.](#)
326 [Yang, W., Cao, J., Wu, Y., Kong, F., and Li, L.: Review on plant terpenoid emissions](#)
327 [worldwide and in China, The Science of the total environment, 787, 147454-147454,](#)
328 [10.1016/j.scitotenv.2021.147454, 2021.](#)
329 [Zhang, J., An, J., Qu, Y., Liu, X., and Chen, Y.: Impacts of potential HONO sources on the](#)
330 [concentrations of oxidants and secondary organic aerosols in the Beijing-Tianjin-Hebei](#)
331 [region of China, Science of the Total Environment, 647, 836-852,](#)
332 [10.1016/j.scitotenv.2018.08.030, 2019a.](#)
333 [Zhang, P., Chen, T., Liu, J., Liu, C., Ma, J., Ma, Q., Chu, B., and He, H.: Impacts of SO₂,](#)
334 [Relative Humidity, and Seed Acidity on Secondary Organic Aerosol Formation in the](#)
335 [Ozonolysis of Butyl Vinyl Ether, Environmental Science & Technology, 53, 8845-8853,](#)
336 [10.1021/acs.est.9b02702, 2019b.](#)
337 [Zhang, Y.-Q., Chen, D.-H., Ding, X., Li, J., Zhang, T., Wang, J.-Q., Cheng, Q., Jiang, H.,](#)
338 [Song, W., Ou, Y.-B., Ye, P.-L., Zhang, G., and Wang, X.-M.: Impact of anthropogenic](#)
339 [emissions on biogenic secondary organic aerosol: observation in the Pearl River Delta,](#)
340 [southern China, Atmospheric Chemistry and Physics, 19, 14403-14415, 10.5194/acp-19-](#)
341 [14403-2019, 2019c.](#)
342 [Zhang, Y., Chen, Y., Lei, Z., Olson, N. E., Riva, M., Koss, A. R., Zhang, Z., Gold, A., Jayne,](#)
343 [J. T., Worsnop, D. R., Onasch, T. B., Kroll, J. H., Turpin, B. J., Ault, A. P., and Surratt,](#)
344 [J. D.: Joint Impacts of Acidity and Viscosity on the Formation of Secondary Organic](#)
345 [Aerosol from Isoprene Epoxydiols \(IEPDX\) in Phase Separated Particles, Acs Earth and](#)
346 [Space Chemistry, 3, 2646-2658, 10.1021/acsearthspacechem.9b00209, 2019d.](#)
347 [Zhao, D. F., Schmitt, S. H., Wang, M. J., Acir, I. H., Tillmann, R., Tan, Z. F., Novelli, A.,](#)
348 [Fuchs, H., Pullinen, I., Wegener, R., Rohrer, F., Wildt, J., Kiendler-Scharr, A., Wahner,](#)
349 [A., and Mentel, T. F.: Effects of NO_x and SO₂ on the secondary organic aerosol](#)
350 [formation from photooxidation of alpha-pinene and limonene, Atmospheric Chemistry](#)
351 [and Physics, 18, 1611-1628, 10.5194/acp-18-1611-2018, 2018.](#)

352 [Zheng, G., Su, H., Wang, S., Andreae, M. O., Poschl, U., and Cheng, Y.: Multiphase buffer](#)
353 [theory explains contrasts in atmospheric aerosol acidity, *Science*, 369, 1374-+,](#)
354 [10.1126/science.aba3719, 2020.](#)

355 [Zhou, M., Zheng, G., Wang, H., Qiao, L., Zhu, S., Huang, D., An, J., Lou, S., Tao, S., Wang,](#)
356 [Q., Yan, R., Ma, Y., Chen, C., Cheng, Y., Su, H., and Huang, C.: Long-term trends and](#)
357 [drivers of aerosol pH in eastern China, *Atmos. Chem. Phys. Discuss.*, 2021, 1-21,](#)
358 [10.5194/acp-2021-455, 2021.](#)

359 [Zhu, J., Penner, J. E., Yu, F., Sillman, S., Andreae, M. O., and Coe, H.: Decrease in radiative](#)
360 [forcing by organic aerosol nucleation, climate, and land use change, *Nature*](#)
361 [Communications](#), 10, 10.1038/s41467-019-08407-7, 2019.

362 [Charan, S.M., Huang, Y., Seinfeld, J.H., 2019. Computational Simulation of Secondary](#)
363 [Organic Aerosol Formation in Laboratory Chambers. *Chem. Rev.* 119, 11912-11944.](#)

364 [Cheng, Y., Ma, Y., Hu, D., 2021. Traacer-based source apportioning of atmospheric organic](#)
365 [carbon and the influence of anthropogenic emissions on secondary organic aerosol](#)
366 [formation in Hong Kong. *Atmos. Chem. Phys.* 21, 10589-10608.](#)

367 [Dhulipala, S.V., Bhandari, S., Hildebrandt Ruiz, L., 2019. Formation of oxidized organic](#)
368 [compounds from Cl-initiated oxidation of toluene. *Atmospheric Environment* 199, 265-](#)
369 [273.](#)

370 [Ding, X., He, Q. F., Shen, R. Q., Yu, Q. Q., Wang, X. M., 2014. Spatial distributions of](#)
371 [secondary organic aerosols from isoprene, monoterpenes, beta-caryophyllene, and](#)
372 [aromatics over China during summer. *Journal of Geophysical Research Atmospheres*](#)
373 [119, 11877-11891.](#)

374 [Friese, E., Ebel, A., 2010. Temperature-Dependent Thermodynamic Model of the System](#)
375 [H⁺-NH₄⁺-Na⁺-SO₄²⁻-NO₃⁻-Cl⁻-H₂O. *The Journal of Physical Chemistry A* 114,](#)
376 [11595-11631.](#)

377 [Fu, P., Kawamura, K., Chen, J., Barrie, L.A., 2009. Isoprene, Monoterpene, and](#)
378 [Sesquiterpene Oxidation Products in the High Arctic Aerosols during Late Winter to](#)
379 [Early Summer. *Environmental Science & Technology* 43, 4022-4028.](#)

380 [Guo, H., Weber, R.J., Nenes, A., 2017. High levels of ammonia do not raise fine particle pH](#)
381 [sufficiently to yield nitrogen-oxide-dominated sulfate production. *Scientific Reports* 7,](#)
382 [12109.](#)

383 [Hallquist, M., Wenger, J.C., Baltensperger, U., Rudich, Y., Simpson, D., Claeys, M.,](#)
384 [Dommen, J., Donahue, N.M., George, C., Goldstein, A.H., Hamilton, J.F., Herrmann, H.,](#)
385 [Hoffmann, T., Iinuma, Y., Jang, M., Jenkin, M.E., Jimenez, J.L., Kiendler-Scharr, A.,](#)
386 [Maenhaut, W., McFiggans, G., Mentel, T.F., Monod, A., Prevot, A.S.H., Seinfeld, J.H.,](#)
387 [Surratt, J.D., Szmigielski, R., Wildt, J., 2009. The formation, properties and impact of](#)
388 [secondary organic aerosol: current and emerging issues. *Atmospheric Chemistry and*](#)
389 [Physics](#) 9, 5155-5236.

390 Hao, L., Kari, E., Leskinen, A., Worsnop, D.R., Virtanen, A., 2020. Direct contribution of
391 ammonia to α -pinene secondary organic aerosol formation. *Atmos. Chem. Phys.* 20,
392 14393-14405.

393 Hong, Y., Xu, X., Liao, D., Zheng, R., Ji, X., Chen, Y., Xu, L., Li, M., Wang, H., Xiao, H.,
394 Choi, S.-D., Chen, J., 2021. Source apportionment of PM_{2.5} and sulfate formation
395 during the COVID-19 lockdown in a coastal city of southeast China. *Environmental*
396 *Pollution* 286, 117577.

397 Hong, Z., Zhang, H., Zhang, Y., Xu, L., Liu, T., Xiao, H., Hong, Y., Chen, J., Li, M., Deng,
398 J., Wu, X., Hu, B., Chen, X., 2019. Secondary organic aerosol of PM_{2.5} in a
399 mountainous forest area in southeastern China: Molecular compositions and tracers
400 implication. *Science of the Total Environment* 653, 496-503.

401 Hoyle, C.R., Boy, M., Donahue, N.M., Fry, J.L., Glasius, M., Guenther, A., Hallar, A.G.,
402 Hartz, K.H., Petters, M.D., Petaja, T., Rosenoern, T., Sullivan, A.P., 2011. A review of
403 the anthropogenic influence on biogenic secondary organic aerosol. *Atmospheric*
404 *Chemistry and Physics* 11, 321-343.

405 Hu, B., Liu, T., Hong, Y., Xu, L., Li, M., Wu, X., Wang, H., Chen, J., Chen, J., 2020.
406 Characteristics of peroxyacetyl nitrate (PAN) in a coastal city of southeastern China:
407 Photochemical mechanism and pollution process. *Science of the Total Environment* 719.

408 Jaoui, M., Kleindienst, T.E., Lewandowski, M., Offenberg, J.H., Edney, E.O., 2005.
409 Identification and quantification of aerosol polar oxygenated compounds bearing
410 carboxylic or hydroxyl groups. 2. Organic tracer compounds from monoterpenes.
411 *Environmental Science & Technology* 39, 5661-5673.

412 Jaoui, M., Lewandowski, M., Kleindienst, T.E., Offenberg, J.H., Edney, E.O., 2007. β -
413 caryophyllinic acid: An atmospheric tracer for β -caryophyllene secondary organic
414 aerosol. *Geophysical Research Letters* 34.

415 Kari, E., Hao, L.Q., Ylisirnio, A., Buchholz, A., Leskinen, A., Yli-Pirila, P., Nuutinen, I.,
416 Kuusalo, K., Jokiniemi, J., Faiola, C.L., Schobesberger, S., Virtanen, A., 2019.
417 Potential dual effect of anthropogenic emissions on the formation of biogenic secondary
418 organic aerosol (BSOA). *Atmospheric Chemistry and Physics* 19, 15651-15671.

419 Kleindienst, T.E., Jaoui, M., Lewandowski, M., Offenberg, J.H., Lewis, C.W., Bhave, P.V.,
420 Edney, E.O., 2007. Estimates of the contributions of biogenic and anthropogenic
421 hydrocarbons to secondary organic aerosol at a southeastern US location. *Atmospheric*
422 *Environment* 41, 8288-8300.

423 Lewandowski, M., Piletic, I.R., Kleindienst, T.E., Offenberg, J.H., Beaver, M.R., Jaoui, M.,
424 Docherty, K.S., Edney, E.O., 2013. Secondary organic aerosol characterisation at field-

425 sites across the United States during the spring-summer period. *International Journal of*
426 *Environmental Analytical Chemistry* 93, 1084-1103.

427 Liu, S., Huang, D., Wang, Y., Zhang, S., Wu, C., Du, W., Wang, G., 2021. Synergetic effect
428 of NH₃ and NO_x on the production and optical absorption of secondary organic aerosol
429 formation from toluene photooxidation. *Atmos. Chem. Phys.* 21, 17759-17773.

430 Liu, S., Tsona, N.T., Zhang, Q., Jia, L., Xu, Y., Du, L., 2019. Influence of relative humidity
431 on cyclohexene SOA formation from OH photooxidation. *Chemosphere* 231, 478-486.

432 Liu, T., Hu, B., Xu, X., Hong, Y., Zhang, Y., Wu, X., Xu, L., Li, M., Chen, Y., Chen, X.,
433 Chen, J., 2020. Characteristics of PM_{2.5} bound secondary organic aerosol tracers in a
434 coastal city in Southeastern China: Seasonal patterns and pollution identification.
435 *Atmospheric Environment* 237.

436 Luo, H., Jia, L., Wan, Q., An, T., Wang, Y., 2019. Role of liquid water in the formation of O
437 3 and SOA particles from 1,2,3-trimethylbenzene. *Atmospheric Environment* 217.

438 Lv, S., Wang, F., Wu, C., Chen, Y., Liu, S., Zhang, S., Li, D., Du, W., Zhang, F., Wang, H.,
439 Huang, C., Fu, Q., Duan, Y., Wang, G., 2022. Gas-to-Aerosol Phase Partitioning of
440 Atmospheric Water-Soluble Organic Compounds at a Rural Site in China: An Enhancing
441 Effect of NH₃ on SOA Formation. *Environmental Science & Technology*.

442 Ma, Q., Lin, X.X., Yang, C.G., Long, B., Gai, Y.B., Zhang, W.J., 2018. The influences of
443 ammonia on aerosol formation in the ozonolysis of styrene: roles of Criegee intermediate
444 reactions. *Roy Soc Open Sci* 5.

445 Mahilang, M., Deb, M.K., Pervez, S., 2021. Biogenic secondary organic aerosols: A review
446 on formation mechanism, analytical challenges and environmental impacts.
447 *Chemosphere* 262.

448 McFiggans, G., Mentel, T.F., Wildt, J., Pullinen, I., Kang, S., Kleist, E., Schmitt, S., Springer,
449 M., Tillmann, R., Wu, C., Zhao, D.F., Hallquist, M., Faxon, C., Le Breton, M., Hallquist,
450 A.M., Simpson, D., Bergstrom, R., Jenkin, M.E., Ehn, M., Thornton, J.A., Alfarra, M.R.,
451 Bannan, T.J., Percival, C.J., Priestley, M., Topping, D., Kiendler-Seharr, A., 2019.
452 Secondary organic aerosol reduced by mixture of atmospheric vapours. *Nature* 565, 587-
453 593.

454 Na, K., Song, C., Switzer, C., Cocker, D.R., 2007. Effect of Ammonia on Secondary Organic
455 Aerosol Formation from α -Pinene Ozonolysis in Dry and Humid Conditions.
456 *Environmental Science & Technology* 41, 6096-6102.

457 Newland, M.J., Bryant, D.J., Dunmore, R.E., Bannan, T.J., Acton, W.J.F., Langford, B.,
458 Hopkins, J.R., Squires, F.A., Dixon, W., Drysdale, W.S., Ivatt, P.D., Evans, M.J.,
459 Edwards, P.M., Whalley, L.K., Heard, D.E., Slater, E.J., Woodward-Massey, R., Ye, C.,
460 Mehra, A., Worrall, S.D., Bacak, A., Coc, H., Percival, C.J., Hewitt, C.N., Lee, J.D., Cui,

461 T., Surratt, J.D., Wang, X., Lewis, A.C., Rickard, A.R., Hamilton, J.F., 2021. Low NO_x-
462 atmospheric oxidation pathways in a polluted megacity. *Atmos. Chem. Phys.* 21, 1613-
463 1625.

464 Offenberg, J.H., Lewandowski, M., Edney, E.O., Kleindienst, T.E., Jaoui, M., 2009. Influence
465 of Aerosol Acidity on the Formation of Secondary Organic Aerosol from Biogenic-
466 Precursor Hydrocarbons. *Environmental Science & Technology* 43, 7742-7747.

467 Offenberg, J.H., Lewis, C.W., Lewandowski, M., Jaoui, M., Kleindienst, T.E., Edney, E.O.,
468 2007. Contributions of toluene and alpha-pinene to SOA formed in an irradiated-
469 toluene/alpha-pinene/NO_x/air mixture: Comparison of results using C-14 content and
470 SOA organic tracer methods. *Environmental Science & Technology* 41, 3972-3976.

471 Palmer, P.I., Marvin, M.R., Siddans, R., Kerridge, B.J., Moore, D.P., 2022. Nocturnal
472 survival of isoprene linked to formation of upper tropospheric organic aerosol. *Science*-
473 375, 562-566.

474 Reid, J.P., Bertram, A.K., Topping, D.O., Laskin, A., Martin, S.T., Petters, M.D., Pope, F.D.,
475 Rovelli, G., 2018. The viscosity of atmospherically relevant organic particles. *Nature*-
476 *Communications* 9.

477 Riva, M., Budisulistiorini, S.H., Zhang, Z., Gold, A., Surratt, J.D., 2016. Chemical-
478 characterization of secondary organic aerosol constituents from isoprene ozonolysis in
479 the presence of acidic aerosol. *Atmospheric Environment* 130, 5-13.

480 Sarrafzadeh, M., Wildt, J., Pullinen, I., Springer, M., Kleist, E., Tillmann, R., Schmitt, S.H.,
481 Wu, C., Mentel, T.F., Zhao, D., Hastie, D.R., Kiendler-Scharr, A., 2016. Impact of NO_x-
482 and OH on secondary organic aerosol formation from beta-pinene photooxidation.-
483 *Atmospheric Chemistry and Physics* 16, 11237-11248.

484 Shrivastava, M., Andreae, M.O., Artaxo, P., Barbosa, H.M.J., Berg, L.K., Brito, J., Ching, J.,
485 Easter, R.C., Fan, J., Fast, J.D., Feng, Z., Fuentes, J.D., Glasius, M., Goldstein, A.H.,
486 Alves, E.G., Gomes, H., Gu, D., Guenther, A., Jathar, S.H., Kim, S., Liu, Y., Lou, S.,
487 Martin, S.T., McNeill, V.F., Medeiros, A., de Sa, S.S., Shilling, J.E., Springston, S.R.,
488 Souza, R.A.F., Thornton, J.A., Isaacman VanWertz, G., Yee, L.D., Ynoue, R., Zaveri,
489 R.A., Zelenyuk, A., Zhao, C., 2019. Urban pollution greatly enhances formation of
490 natural aerosols over the Amazon rainforest. *Nature Communications* 10.

491 Shrivastava, M., Cappa, C.D., Fan, J., Goldstein, A.H., Guenther, A.B., Jimenez, J.L., Kuang,
492 C., Laskin, A., Martin, S.T., Ng, N.L., Petaja, T., Pierce, J.R., Rasch, P.J., Roldin, P.,
493 Seinfeld, J.H., Shilling, J., Smith, J.N., Thornton, J.A., Volkamer, R., Wang, J.,
494 Worsnop, D.R., Zaveri, R.A., Zelenyuk, A., Zhang, Q., 2017. Recent advances in
495 understanding secondary organic aerosol: Implications for global climate forcing.-
496 *Reviews of Geophysics* 55, 509-559.

497 Song, M., Zhang, C., Wu, H., Mu, Y., Ma, Z., Zhang, Y., Liu, J., Li, X., 2019. The influence
498 of OH concentration on SOA formation from isoprene photooxidation. *Science of the*
499 *Total Environment* 650, 951-957.

500 Surratt, J.D., Chan, A.W.H., Eddingsaas, N.C., Chan, M., Loza, C.L., Kwan, A.J., Hersey,
501 S.P., Flagan, R.C., Wennberg, P.O., Seinfeld, J.H., 2010. Reactive intermediates
502 revealed in secondary organic aerosol formation from isoprene. *Proceedings of the*
503 *National Academy of Sciences of the United States of America* 107, 6640-6645.

504 Surratt, J.D., Lewandowski, M., Offenberg, J.H., Jaoui, M., Kleindienst, T.E., Edney, E.O.,
505 Seinfeld, J.H., 2007. Effect of acidity on secondary organic aerosol formation from
506 isoprene. *Environmental Science & Technology* 41, 5363-5369.

507 Wang, D.S., Ruiz, L.H., 2017. Secondary organic aerosol from chlorine initiated oxidation of
508 isoprene. *Atmos. Chem. Phys.* 17, 13491-13508.

509 Wang, J., Ye, J., Zhang, Q., Zhao, J., Wu, Y., Li, J., Liu, D., Li, W., Zhang, Y., Wu, C., Xie,
510 C., Qin, Y., Lei, Y., Huang, X., Guo, J., Liu, P., Fu, P., Li, Y., Lee, H.C., Choi, H.,
511 Zhang, J., Liao, H., Chen, M., Sun, Y., Ge, X., Martin, S.T., Jacob, D.J., 2021a. Aqueous
512 production of secondary organic aerosol from fossil-fuel emissions in winter Beijing
513 haze. *Proceedings of the National Academy of Sciences of the United States of America*
514 118.

515 Wang, J., Ye, J., Zhang, Q., Zhao, J., Wu, Y., Li, J., Liu, D., Li, W., Zhang, Y., Wu, C., Xie,
516 C., Qin, Y., Lei, Y., Huang, X., Guo, J., Liu, P., Fu, P., Li, Y., Lee, H.C., Choi, H.,
517 Zhang, J., Liao, H., Chen, M., Sun, Y., Ge, X., Martin, S.T., Jacob, D.J., 2021b. Aqueous
518 production of secondary organic aerosol from fossil-fuel emissions in winter Beijing
519 haze. *Proc Natl Acad Sci U S A* 118.

520 Wang, S., Du, L., Tsona, N.T., Jiang, X., You, B., Xu, L., Yang, Z., Wang, W., 2020. Effect
521 of NO_x and SO₂ on the photooxidation of methylglyoxal: Implications in secondary
522 aerosol formation. *J Environ Sci (China)* 92, 151-162.

523 Wang, X., Jacob, D.J., Downs, W., Zhai, S., Zhu, L., Shah, V., Holmes, C.D., Sherwen, T.,
524 Alexander, B., Evans, M.J., Eastham, S.D., Neuman, J.A., Veres, P.R., Koenig, T.K.,
525 Volkamer, R., Huey, L.G., Bannan, T.J., Percival, C.J., Lee, B.H., Thornton, J.A., 2021c.
526 Global tropospheric halogen (Cl, Br, I) chemistry and its impact on oxidants. *Atmos.*
527 *Chem. Phys.* 21, 13973-13996.

528 Wen, L., Chen, T., Zheng, P., Wu, L., Wang, X., Mellouki, A., Xue, L., Wang, W., 2019.
529 Nitrous acid in marine boundary layer over eastern Bohai Sea, China: Characteristics,
530 sources, and implications. *Sci. Total Environ.*

531 Wu, X., Li, M., Chen, J., Wang, H., Xu, L., Hong, Y., Zhao, G., Hu, B., Zhang, Y., Dan, Y.,
532 Yu, S., 2020. The characteristics of air pollution induced by the quasi-stationary front:
533 Formation processes and influencing factors. *Science of the Total Environment* 707.
534 Wu, X., Xu, L.L., Hong, Y.W., Chen, J.F., Qiu, Y.Q., Hu, B.Y., Hong, Z.Y., Zhang, Y.R.,
535 Liu, T.T., Chen, Y.T., Bian, Y.H., Zhao, G.Q., Chen, J.S., Li, M.R., 2019. The air-
536 pollution governed by subtropical high in a coastal city in Southeast China: Formation-
537 processes and influencing mechanisms. *Science of the Total Environment* 692, 1135-
538 1145.
539 Xiao, Y., Wu, Z., Guo, S., He, L., Huang, X., Hu, M., 2020. Formation mechanism of-
540 secondary organic aerosol in aerosol liquid water: A review. *Chinese Science Bulletin* 65,
541 3118-3133.
542 Xu, L., Du, L., Tsona, N.T., Ge, M.F., 2021. Anthropogenic Effects on Biogenic Secondary-
543 Organic Aerosol Formation. *Advances in Atmospheric Sciences* 38, 1053-1084.
544 Xu, L., Guo, H., Boyd, C.M., Klein, M., Bougiatioti, A., Cerully, K.M., Hite, J.R., Isaacman-
545 VanWertz, G., Kreisberg, N.M., Knote, C., Olson, K., Koss, A., Goldstein, A.H., Hering,
546 S.V., de Gouw, J., Baumann, K., Lee, S.H., Nenes, A., Weber, R.J., Ng, N.L., 2015.
547 Effects of anthropogenic emissions on aerosol formation from isoprene and-
548 monoterpenes in the southeastern United States. *Proc Natl Acad Sci U S A* 112, 37-42.
549 Yang, W., Cao, J., Wu, Y., Kong, F., Li, L., 2021. Review on plant terpenoid emissions-
550 worldwide and in China. *Science of the total environment* 787, 147454-147454.
551 Zhang, J., An, J., Qu, Y., Liu, X., Chen, Y., 2019a. Impacts of potential HONO sources on the
552 concentrations of oxidants and secondary organic aerosols in the Beijing-Tianjin-Hebei-
553 region of China. *Science of the Total Environment* 647, 836-852.
554 Zhang, P., Chen, T., Liu, J., Liu, C., Ma, J., Ma, Q., Chu, B., He, H., 2019b. Impacts of SO₂-
555 Relative Humidity, and Seed Acidity on Secondary Organic Aerosol Formation in the-
556 Ozonolysis of Butyl Vinyl Ether. *Environmental Science & Technology* 53, 8845-8853.
557 Zhang, Y. Q., Chen, D. H., Ding, X., Li, J., Zhang, T., Wang, J. Q., Cheng, Q., Jiang, H.,
558 Song, W., Ou, Y. B., Ye, P. L., Zhang, G., Wang, X. M., 2019c. Impact of-
559 anthropogenic emissions on biogenic secondary organic aerosol: observation in the Pearl-
560 River Delta, southern China. *Atmospheric Chemistry and Physics* 19, 14403-14415.
561 Zhang, Y., Chen, Y., Lei, Z., Olson, N.E., Riva, M., Koss, A.R., Zhang, Z., Gold, A., Jayne,
562 J.T., Worsnop, D.R., Onasch, T.B., Kroll, J.H., Turpin, B.J., Ault, A.P., Surratt, J.D.,
563 2019d. Joint Impacts of Acidity and Viscosity on the Formation of Secondary Organic-
564 Aerosol from Isoprene Epoxydiols (IEPDX) in Phase Separated Particles. *Acs Earth and*
565 *Space Chemistry* 3, 2646-2658.

566 ~~Zhao, D.F., Schmitt, S.H., Wang, M.J., Acir, I.H., Tillmann, R., Tan, Z.F., Novelli, A., Fuchs,~~
567 ~~H., Pullinen, I., Wegener, R., Rohrer, F., Wildt, J., Kiendler-Sehr, A., Wahner, A.,~~
568 ~~Mentel, T.F., 2018. Effects of NO_x and SO₂ on the secondary organic aerosol formation~~
569 ~~from photooxidation of alpha-pinene and limonene. Atmospheric Chemistry and Physics~~
570 ~~18, 1611-1628.~~

571 ~~Zheng, G., Su, H., Wang, S., Andreae, M.O., Pöschl, U., Cheng, Y., 2020. Multiphase buffer~~
572 ~~theory explains contrasts in atmospheric aerosol acidity. Science 369, 1374 +.~~

573 ~~Zhou, M., Zheng, G., Wang, H., Qiao, L., Zhu, S., Huang, D., An, J., Lou, S., Tao, S., Wang,~~
574 ~~Q., Yan, R., Ma, Y., Chen, C., Cheng, Y., Su, H., Huang, C., 2021. Long term trends and~~
575 ~~drivers of aerosol pH in eastern China. Atmos. Chem. Phys. Discuss. 2021, 1-21.~~

576 ~~Zhu, J., Penner, J.E., Yu, F., Sillman, S., Andreae, M.O., Coe, H., 2019. Decrease in radiative~~
577 ~~forcing by organic aerosol nucleation, climate, and land use change. Nature~~
578 ~~Communications 10.~~

579

580

581